M.Tech (Control & Instrumentation)

Comparative Performance Evaluation of Automotive USB Type-C Power Delivery Charger ICs

A DISSERTATION

SUBMITTED IN PARTIAL FULFILLMENT OF THE REQUIREMENTS

FOR THE AWARD OF THE DEGREE

OF

MASTER OF TECHNOLOGY

IN

CONTROL & INSTRUMENTATION

Submitted by:

DHRATIKA SINGH

24/C&I/22

Under the supervision of

Dr. MADHUSUDAN SINGH

Dr. MINI SREEJETH

(Professor, EED, DTU)

DEPARTMENT OF ELECTRICAL ENGINEERING

DELHI TECHNOLOGICAL UNIVERSITY

(Formerly Delhi College of Engineering)

Bawana Road, Delhi-110042

MAY, 2026

DHRATIKA SINGH

2026

DELHI TECHNOLOGICAL UNIVERSITY
(Formerly Delhi College of Engineering)
Bawana Road, Delhi-110042

CANDIDATE'S DECLARATION

I Dhratika Singh, 24/C&I/22 student of M.Tech (Control & Instrumentation), hereby declare that the project dissertation titled "Comparative Performance Evaluation of Automotive USB Type-C Power Delivery Charger ICs" which is submitted by me to the Department of Electrical Engineering, Delhi Technological University, Delhi in partial fulfilment of the requirement for the award of the degree of Master of Technology, an original work and has not been copied from any source without proper acknowledgement and citation. This work has not previously formed the basis for the award of any degree, diploma, associateship, fellowship or other similar title or recognition.

Place: Delhi Dhratika Singh
Date:

DELHI TECHNOLOGICAL UNIVERSITY
(Formerly Delhi College of Engineering)
Bawana Road, Delhi-110042

CERTIFICATE

I hereby declare that the Project Dissertation titled "Comparative Performance Evaluation of Automotive USB Type-C Power Delivery Charger ICs" which is submitted by Dhratika Singh, 24/C&I/22 Department of Electrical Engineering, Delhi Technological University, Delhi, in partial fulfilment of the requirement for the award of the degree of Master of Technology, is a record of the project work carried out by the student under my supervision. This work has not been submitted in part or in full for any Degree or Diploma to this University or elsewhere.

Place: Delhi
Date:

SUPERVISOR
Dr Mini Sreejeth
Professor, EED
DTU, Delhi

ACKNOWLEDGEMENT

I sincerely thank my supervisor, Dr. Mini Sreejeth, from the Department of Electrical Engineering at Delhi Technological University, for her invaluable guidance, constant encouragement, and technical support during this thesis. Her insightful suggestions and motivation significantly helped me complete this research successfully.

I am grateful to the faculty and lab staff in the Department of Electrical Engineering at Delhi Technological University for providing the facilities and academic environment I needed to complete this work.

I appreciate Ola Electric Technologies for providing me with hands-on industry experience and for helping me understand automotive USB Type-C Power Delivery charging systems and testing methods.

Finally, I would like to thank my family and friends for always supporting, encouraging, and motivating me during my M. Tech, and while I completed this thesis.

DHRATIKA SINGH
Department of Electrical Engineering
Delhi Technological University

ABSTRACT

Automotive charging systems in EV two-wheelers operate under continuously changing battery and load conditions during real-time usage. In an EV scooter cluster, integrating wired smartphone charging requires the charging system to deliver stable performance, high efficiency, and reliable protection across different operating conditions. USB Type-C Power Delivery (USB PD) technology has become a suitable solution for such applications because it supports fast charging and flexible power delivery.

The thesis focuses on three automotive USB PD charging ICs: the Injoinic IC from Injoinic Technology, the power delivery evaluation board from Monolithic Power Systems, and the Renesas evaluation board featuring a three-level buck converter integrated.

The Injoinic IC charger circuit was implemented on a 5-inch TFT display board using a custom schematic designed in Cadence software for the S1X cluster PCB. At the same time, the MPS and Renesas devices were evaluated using dedicated evaluation boards.

Hardware testing was carried out using laboratory instruments, including a DC power supply, an electronic DC load, a DSO and a USB PD analyser for protocol detection. USB PD negotiation and protocol analysis were performed using a PD sink trigger board and Charger LAB PD analyzer.

Hardware testing mainly included efficiency measurements at different load currents, protocol verification, and protection validation under various USB PD voltage profiles. Performance characterisation was carried out under PDO operation at 5V, 9V, and 12V.

The MPS evaluation board demonstrates higher efficiency and greater configurability via the Virtual Bench Pro software interface when testing the charger IC across different voltage profiles. The Injoinic IC offered a compact, integrated charging solution suitable

for integration into TFT displays. Initial testing of the Renesas board is for higher-power applications in laptops. However, further validation was not possible due to hardware damage.

Experimental measurements indicated that passive component selection and output voltage profiles significantly influence the buck converter's efficiency, switching behaviour, and thermal performance.

The results were utilised to compare the practical implementation, protocol capabilities, efficiency characteristics, and protection behaviour of various automotive USB PD charging.

CONTENTS

CANDIDATE'S DECLARATION	i
CERTIFICATE	ii
ACKNOWLEDGEMENT	iii
ABSTRACT	iv
CONTENTS	v
LIST OF FIGURES	vi
LIST OF TABLES	vii
LIST OF ABBREVIATIONS	viii
CHAPTER 1 – INTRODUCTION	13
1.1 Background	13
1.2 Motivation for the work	14
1.3 Problem statement	14
1.4 Objective of the work	15
1.5 Scope of the work	15
1.6 Organization of thesis	16
CHAPTER 2 - LITERATURE REVIEW	17
2.1 Introduction	17
2.2 Evolution of USB charging technologies	18
2.3 Battery Charging Specifications (BC1.2)	19
2.4 Quick Charge Technologies	20
2.5 USB Type-C Connector Architecture	21
2.6 Configuration Channel Communication	22
2.7 USB PD Voltage Profiles	22
2.8 Programmable Power Supply (PPS)	23
2.9 USB PD Communication and Negotiation	24
2.10 DP/DM Based Charging Communication	25
2.11 Conclusion	25
CHAPTER 3 - HARDWARE EXPERIMENTAL SETUP	26
3.1 Automotive USB PD Charging System Architecture	26
3.2 Injoinic IC Architecture and Operating Principle	26
3.2.1 Injoinic IC Internal Architecture	27
3.2.2 Injoinic IC Functional Description	28
3.2.3 Schematic Design of Injoinic IC-Based USB PD Charger	29
3.2.4 Input Power Stage Design	29
3.2.5 Buck Converter Power Stage	30
3.2.6 Output Configuration and Passive Component Design	31
3.2.7 TFT Display Board Integration	31
3.3 MPS Evaluation Board Architecture	32
3.3.1 MPS Internal Architecture	34
3.3.2 Functional Description of MPS	35
3.3.3 Virtual Bench Pro Configuration	36
3.3.4 Protection Features	38
3.4 Renesas Evaluation Board	37
3.4.1 3-Level Buck Converter Architecture	38
3.4.2 Renesas Board USB Type-C Port Controller	39
3.5 Comparative Hardware Analysis of Selected Charger Ics	40

3.6 Conclusion 41
CHAPTER 4 - EXPERIMENTAL ANALYSIS 42
4.1 Experimental Test Setup 42
4.1.1 Overall Hardware Test Bench 43
4.1.2 USB PD Sink Trigger Board Configuration 43
4.1.3 Charger LAB Protocol Analyzer Setup 44
4.2 USB PD Voltage Profile Configuration 46
4.3. Experimental Evaluation of Injoinic IC 48
4.4 Load Regulation Testing for Injoinic IC 51
4.5 Experimental Evaluation of MPS Board 55
4.6 Load Regulation Testing for MPS Board 56
4.7 Experimental Evaluation of Renesas Board 58
4.8 Load Regulation Testing for Renesas Board 60
4.9 Protection Testing 61
4.10 Conclusion 65
CHAPTER 5 - COMPARATIVE ANALYSIS AND CONCLUSION 66
5.1 Comparative Analysis of Automotive USB PD 66
5.2 Conclusion 67
5.3 Future Scope 67
REFERENCE

LIST OF FIGURES

Figure 2.1: Evolution of USB Charging Technologies 18
Figure 2.2: QC Voltage Negotiation through DP/DM communication 20
Figure 2.3: USB Type-C Connector Pin Diagram 21
Figure 2.4: CC Communication and Connection Detection 22
Figure 3.1: Overall architecture of the implemented USB PD charging system 26
Figure 3.2: Pin Diagram of Injoinic IC 27
Figure 3.3: Functional Internal Architecture of Injoinic IC 28
Figure 3.4: Functional flow diagram of Injoinic IC 28
Figure 3.5: Injoinic IC Schematic Designed in Cadence 29
Figure 3.6: Injoinic IC Input LC Filter and Protection Circuit 30
Figure 3.7: Injoinic IC Buck Converter Power Stage 30
Figure 3.8: Injoinic IC Passive Component Placement in Schematic 31
Figure 3.9: 5-Inch TFT Display Control Board with Injoinic IC 32
Figure 3.10: Front side of MPS Evaluation Board 33
Figure 3.11: Rear side of MPS Evaluation Board 33
Figure 3.12: Internal Functional Architecture of MPS Evaluation Board 34
Figure 3.13: Application Circuit of MPS IC USB PD Controller 35
Figure 3.14: Virtual Bench Pro Interface Used for MPS Configuration 36
Figure 3.15: Front view of Renesas Evaluation Board 37
Figure 3.16: Rear view of Renesas Evaluation Board 37
Figure 3.17: 3-Level Buck Converter Topology in Renesas 38
Figure 3.18: RAA489300 Internal Functional Architecture 39
Figure 4.1: Hardware Setup for USB PD Performance Evaluation 42
Figure 4.2: Front view of USB PD sink trigger module 43
Figure 4.3: Rear view of USB PD sink trigger module 44
Figure 4.4: PD analyzer USB PD Output Monitoring 45
Figure 4.5: PD analyzer VBUS and IBUS Monitoring 45
Figure 4.6: PD analyzer CC Line Monitoring 45
Figure 4.7: PD analyzer PPS Output Monitoring (15W) 46
Figure 4.8: PD analyzer PPS Output Monitoring (12W) 47
Figure 4.9: PD analyzer USB PD Monitoring (20W) 47
Figure 4.10: Injoinic IC Efficiency at 27W and 16V Vin 48

Figure 4.11: Injoinic IC Efficiency at 27W and 29.3V Vin 49
Figure 4.12: Injoinic IC Efficiency at 36W and 12V Vin 49
Figure 4.13: Injoinic IC Efficiency at 48W and 16V Vin 50
Figure 4.14: Injoinic IC Efficiency at 36W and 26V Vin 50
Figure 4.15: Injoinic IC Load Regulation at 27W 51
Figure 4.16: Injoinic IC Load Regulation at 29.3W 52
Figure 4.17: Injoinic IC Load Regulation at 36W 52
Figure 4.18: Injoinic IC Load Regulation at 48W 53
Figure 4.19: Injoinic Load Regulation at 36W (High VIN) 53
Figure 4.20: Injoinic Efficiency with Parallel Inductor Configuration 54
Figure 4.21: Injoinic Efficiency with Series Low DCR Inductor Configuration 54
Figure 4.22: Efficiency Characteristics of MPS Board at 36W 55
Figure 4.23: Efficiency Characteristics of MPS Board at 54W 55
Figure 4.24: Efficiency Characteristics of MPS Board at 72W 56
Figure 4.25: Load Regulation Characteristics of MPS Board at 36W 57
Figure 4.26: Load Regulation Characteristics of MPS Board at 72W 57
Figure 4.27: Efficiency Characteristics of Renesas Board at 84W 58
Figure 4.28: Efficiency Characteristics of Renesas Board at 108W 59
Figure 4.29: Efficiency Characteristics of Renesas Board at 140W 59
Figure 4.30: Load Regulation Characteristics of Renesas Board at 84W 60
Figure 4.31: Load Regulation Characteristics of Renesas Board at 140W 60
Figure 4.32: Load Regulation Characteristics of Renesas Board at 108W 61
Figure 4.33: SC Protection Response of Injoinic IC Observed on Oscilloscope 62
Figure 4.34: Input Under Voltage Protection (UVP) Response of Injoinic IC 62
Figure 4.35: Output UVP and Hiccup Restart Response of Injoinic IC 63
Figure 4.36: DP Pin Over Voltage Protection Response of Injoinic IC 63
Figure 4.37: CC Pin Over Voltage Protection Response of Injoinic IC 64
Figure 4.38: Input Under Voltage Protection Testing of MPS IC 64
Figure 4.39: Input Over Voltage Protection Testing of MPS IC 65

LIST OF TABLES

Table 2.1: Comparison of Fast Charging Protocols 17

Table 2.2: Conventional USB Power Ratings 19

Table 2.3: BC1.2 Port Types 19

Table 2.4: Comparison of Qualcomm Quick Charge Versions 20

Table 2.5: USB PD Voltages, Profiles and Power Capability 23

Table 2.6: Comparison between fixed PDO and PPS Operation 24

Table 2.7: Typical PPS Voltage Ranges and Application 24

Table 3.2: Hardware Comparison of Selected USB PD Charger ICs 40

Table 4.1: CH224K PD Trigger Voltage Selection Table 44

Table 5.1: Performance Comparison of USB PD 66

LIST OF ABBREVIATIONS

Abbreviation	Meaning
USB	Universal Serial Bus
PPS	Programmable Power Supply
CC	Configuration Channel
BMC	Biphase Mark Coding
PDO	Power Data Object
APDO	Adjustable Power Data Object
EPR	Extended Power Range
SPR	Standard Power Range
VBUS	USB Power Bus
DP/DM	Data Positive / Data Minus
EMI	Electromagnetic Interference
EMC	Electromagnetic Compatibility
MPS	Monolithic Power Systems
AEC-Q100	Automotive Electronics Council Qualification Standard
CCM	Continuous Conduction Mode

CHAPTER 1 - INTRODUCTION

1.1 Background

The growing use of smartphones, infotainment systems, navigation devices, and portable electronics in modern vehicles has driven demand for efficient USB charging technologies [1]. Earlier USB charging standards supported only fixed 5V operation with limited power capability, which became insufficient for modern fast-charging devices.

USB Type-C and USB Power Delivery technology offer higher power transfer and programmable voltage negotiation for modern devices [2]. Numerous researchers and semiconductor companies have previously developed USB PD-based fast-charging solutions for portable and automotive uses [3].

Researchers have examined fast-charging converter designs and methods for using USB PD. Yao et al. studied how buck converters operate in USB Power Delivery, focusing on efficiency improvements and current sensing [4]. Bryant and Kazimierczuk explored how buck converters switch and perform under different loads [5].

Recent studies have also looked at USB Type-C Power Delivery communication. Liu et al. examined how to use the USB-PD protocol and design fast-charge controllers for programmable charging [6]. Delshadpour et al. studied the communication architecture and BMC signaling in USB Type-C Power Delivery to ensure reliable communication [7].

Other research has focused on designing efficient USB-C charging converters. Mukherjee et al. explored resonant converter methods to improve efficiency in USB-C Power Delivery [8]. Tran et al. demonstrated how to build a battery charger using a USB Type-C Power Delivery interface for modern charging systems [9].

Automotive charging systems present additional challenges. Automotive charging systems face additional challenges, including changing battery conditions, electrical noise, heat, and the need for compact hardware. Dusmez and Khaligh discussed automotive power electronic systems and highlighted the importance of efficient power conversion and managing heat in vehicles [10]

Injoinic, Monolithic Power Systems (MPS), and Renesas have developed automotive USB PD charger ICs that support programmable-voltage operation, PPS functionality, integrated protection features, and compatibility with multiple charging protocols [11], [12], [13], [14].

However, most available studies mainly focus on theoretical converter analysis or individual charger implementation. Few practical comparisons exist of different automotive USB Type-C Power Delivery charger ICs tested in real lab conditions.

This study aims to evaluate various automotive USB PD charging s at the hardware level, focusing on efficiency, protocol support, protection, thermal performance, and integration with automotive TFT display systems.

1.2 Motivation for the work

Conventional USB charging ports in many automotive systems offer limited power and can't support modern fast-charging smartphones. USB Type-C Power Delivery technology enables higher power transfer and faster charging of portable devices [15].

This work was driven by the need to develop a USB Type-C Power Delivery charging solution for an automotive system with a TFT display, intended for electric two-wheeler applications.

The objective was to develop a compact, efficient charging interface to power mobile devices during vehicle operation. Since automotive systems operate under fluctuating battery voltages and are exposed to electrical noise, thermal variations, and varying load levels, careful selection and evaluation of charger integrated circuits are necessary.

Another motivation for this work was to compare charger behavior through experimental hardware testing.

While datasheets offer theoretical efficiency and protocol details, real- world performance is affected by passive component choices, thermal effects, switching behavior, and load characteristics [16], [17], [18].

Therefore, hardware testing was necessary to evaluate the suitability of different charger ICs for automotive applications.

This work also included schematic design of different ICs so that it is easy for us to compare the all three based on different parameters.

1.3 Problem statement

People want to charge their electric scooters, this is because they use their phones a lot for navigation, talking to friends and listening to music while travelling. Putting a USB Type C fast charger in a small scooter display is not easy.

When building the hardware several problems were found the charger needs to work even when the battery voltage changes while the scooter is in use.

At power, the converter part can get hot, make noise and create voltage ripples. This can affect how well the scooter charges. Also interfere with the nearby TFT board.

Choosing the charger IC was a challenge as some IC supports charging types but need more external parts. When testing it was found that how the converter worked changed based on the parts used, how the circuit board was laid out and the conditions it was used in.

Most of the datasheet just provides the specifications which makes it hard to know which charger IC is best for scooters, without actually testing it.

So the real test of USB type C charger IC was needed. We have to pick a charger that can handle the amount of power for the scooter USB system. In this project we focus on making a 36W USB PD charger that can charge devices in the s1X Electric scooter.

1.4 Objective of the work

The main goal of this project is to try out and see how well USB Type-C Power Delivery charger ICs work for scooters that have a TFT display system.

This project wants to look at how different charger ICs work when you use them with different voltages and loads. The people doing this project picked some ICs.

Look at how well they work, how good they are at keeping the right output, how hot they get and how well they protect things when something goes wrong.

Another thing they wanted to do was check if the USB Power Delivery system works correctly and what kinds of charging protocols it supports.

They used tools to analyze this and see what happens when they change things. They tried out charging modes to see how the converter works when it is actually being used.

The project also wants to compare the charger ICs to see which ones are the best for electric scooters with TFT displays.

They are looking at how complicated the hardware is, if it works with the protocols and if it is a good fit for the electric scooter system. They want to find the best USB Type-C Power Delivery charger ICs for scooters, with TFT display systems.

1.5 Scope of the work

This study looks at how USB Type-C Power Delivery charger ICs work in two-wheelers. It checks how these charging systems do with voltage settings and loads.

USB Power Delivery communication over CC lines and legacy DP/DM-based charging protocol behavior were analyzed using PD analyzer tools.

The scope of the present work is limited to laboratory-level evaluation and does not include automotive EMI/EMC compliance testing, environmental qualification testing, thermal chamber analysis, long-term reliability testing, or production-level hardware optimization.

Advanced automotive qualification testing, such as EMI/EMC compliance, environmental reliability testing, thermal chamber analysis, and large-scale production validation, is beyond the scope of the work.

1.6 Organization of thesis

The document begins with an overview of USB charging technologies, progressing to practical implementation and testing of automotive USB Type-C Power Delivery systems.

The first chapter introduces the background of automotive USB PD charging, as well as the motivation, problem statement, objectives, and scope of the present work.

Chapter 2 covers the development of USB charging technologies, including USB Type-C architecture, USB Power Delivery communication, PPS operation, and automotive charging applications. It also reviews previous research on fast charging and conversion characteristics.

Chapter 3 primarily covers the hardware implementation of the chosen USB PD charging. It discusses the architecture and operation of the Injoinic IC, MPS Board, and Renesas board, including schematic design, power stage setup, communication interfaces, and TFT display integration.

Chapter 4 outlines the experimental setup and testing procedures for practical validation, including efficiency testing, load regulation analysis, protocol verification, and protection testing across various operating conditions.

Finally, Chapter 5 offers a comparative analysis of the chosen chargers, focusing on efficiency, protocol support, implementation complexity, and practical performance. It also includes the conclusion and the future scope of the work that has been discussed.

CHAPTER 2 - LITERATURE REVIEW

2.1 Introduction

Contemporary portable electronic devices require charging systems that deliver higher power, better efficiency, and shorter charging times. Earlier USB charging standards supported fixed-voltage, low-power configurations, which are now inadequate for smartphones, tablets, laptops, and automotive infotainment systems.

Choi et al. investigated the thermal behavior of high-power USB charging systems and determined that converter efficiency and printed circuit board (PCB) thermal management are critical factors influencing charging reliability during continuous operation [18].

Switching performance and electromagnetic interference (EMI) in compact chargers have been the subject of extensive research. Matsuda and Ito analyzed conducted noise in high frequency DC-DC converters and proposed filtering techniques to improve system stability [19]. Wang and Blaabjerg investigated reliability issues arising from thermal and electrical stress [29].

Table 2.1: Comparison of Fast Charging Protocols

Protocol	**Communication Method**	**Voltage Profiles**	**Max Power**
USB 2.0	None	Fixed 5V	2.5W
USB BC1.2	DP/DM	Fixed 5V	7.5W
QC 2.0/3.0	DP/DM	5V / 9V / 12V / 20V	Up to 36W
Samsung AFC	DP/DM	5V / 9V / 12V	Up to 18W
Huawei SCP/FCP	DP/DM	5V / 4.5V / 10V	Up to 40W
USB PD 3.0	CC1 / CC2	5V / 9V / 12V / 15V / 20V	Up to 100W
USB PD 3.1 EPR	CC1 / CC2	28V / 36V / 48V	Up to 240W
PPS	CC1 / CC2	3.3V–21V (Programmable)	Up to 100W

Several studies have also focused on the practical implementation of USB Type-C charging systems. Kim et al. presented compact USB PD charger architectures for portable applications and highlighted the influence of switching frequency and passive component selection on converter efficiency [21].

Although earlier research has examined converter operation and USB PD communication methods, there remains a limited number of practical comparisons of various automotive USB Type-C Power Delivery charger ICs under laboratory conditions. Table 2.1 provides a comparison of fast charging protocols.

Therefore, this work focuses on the experimental evaluation of USB PD chargers with respect to efficiency, protocol capability, thermal behavior, protection performance, and suitability for implementation in automotive TFT display integration.

2.2 Evolution of USB Charging Technologies

USB standards such as USB 1.0 and USB 2.0 were developed for low power data communication and supported limited charging capability at fixed 5V operation only.

USB 2.0 provides a current up to 500mA, enabling around 2.5W of power. As smartphone batteries grew larger and their power needs increased, traditional USB charging no longer sufficed for fast and efficient charging.

To enhance charging performance, a Battery Charging Specification (BC1.2) was created, allowing charging currents up to 1.5A at 5V through dedicated ports.

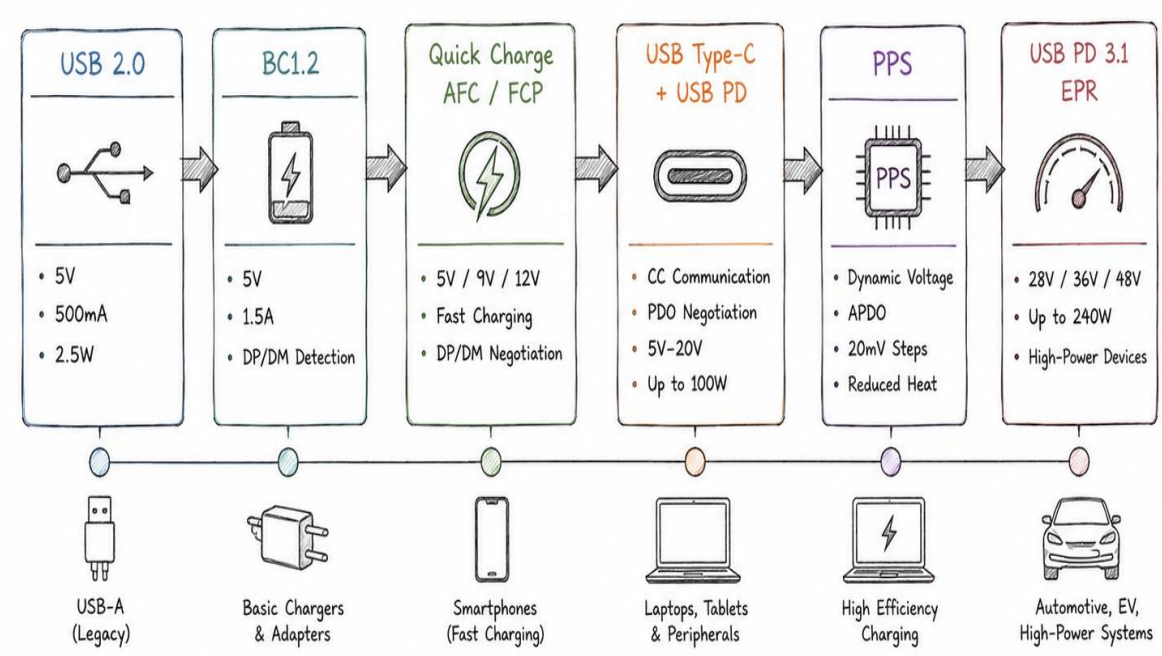

Figure 2.1: Evolution of USB Charging Technologies

Table 2.2: Conventional USB Power Ratings

USB Standard	Output Voltage	Max Current	Max Power	Major Limitation
USB 1.0	5V	100mA	0.5W	Very low charging capability
USB 2.0	5V	500mA	2.5W	Slow charging
USB 3.0	5V	900mA	4.5W	Fixed voltage operation

2.3 Battery Charging Specifications (BC1.2)

To improve power capability beyond conventional USB standards, the USB Implementers introduced the Battery Charging Specification. Earlier USB standards were mainly intended for data communication and supported limited current capability. BC1.2 was later developed to support higher current delivery for smartphones and portable electronic devices.

The BC1.2 specification categorizes USB ports into types such as Standard Downstream Port, Charging Downstream Port, and Dedicated Charging Port. Among these, DCPS support current delivery up to 1.5A, enabling faster charging than traditional USB ports. Refer to table 2.3 for a discussion of BC1.2 port types.

Table 2.3: BC1.2 Port Types

Parameter	Standard Downstream Port	Charging Downstream Port	Dedicated Charging Port
Data Communication Support	Supported	Supported	Not Supported
Voltage	5 V	5 V	5 V
Current Capability	500 mA	1.5 A	1.5 A
Typical Application	PCs, USB devices	Laptops, USB hubs	Wall chargers, adapters
Main Limitation	Slow charging	Fixed 5 V only	No data communication

2.4 Quick Charge Technologies

As smartphone batteries grow larger, standard 5V USB charging is no longer adequate for reducing charging times. As a result, some manufacturers use higher voltage charging to speed up the process. Table 2.4 compares different versions of Qualcomm Quick Charge

Figure 2.2 shows how the communication between the charger and phone works through QC protocol.

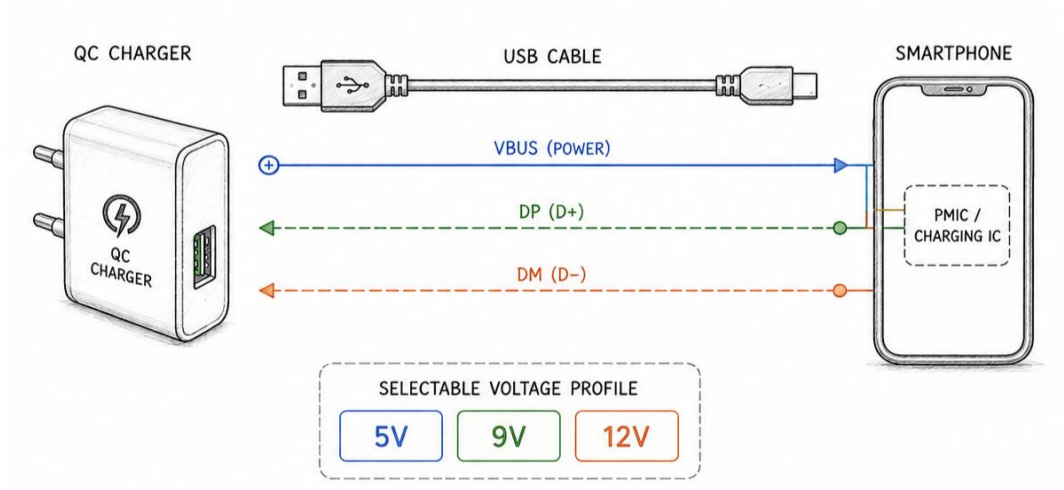

Figure 2.2: QC Voltage Negotiation through DP/DM communication

Table 2.4: Comparison of Qualcomm Quick Charge Versions

QC Version	Output Voltage	Max Power	Communication Method	Feature
QC1.0	5V	10W	DP/DM	Higher current charging
QC2.0	5V/9V/12V	18W	DP/DM voltage signaling	Variable voltage charging
QC3.0	3.6V–20V	18W	INOV algorithm	Dynamic voltage adjustment
QC4/QC4+	USB PD compatible	27W	USB PD + DP/DM	Improved efficiency & thermal performance

2.5 USB Type-C Connector Architecture

USB Type-C is a reversible 24 pin connector unlike earlier USB connectors, the Type-C connector can be inserted in either orientation because of its symmetrical pin arrangement.

Under USB PD 3.1 Extended Power Range (EPR) specifications, the connector can support power delivery up to 48V and 5A operation. The connector contains multiple functional pins including VBUS, GND, CC1, CC2, D+, D−, SBU, and SuperSpeed differential communication pairs.

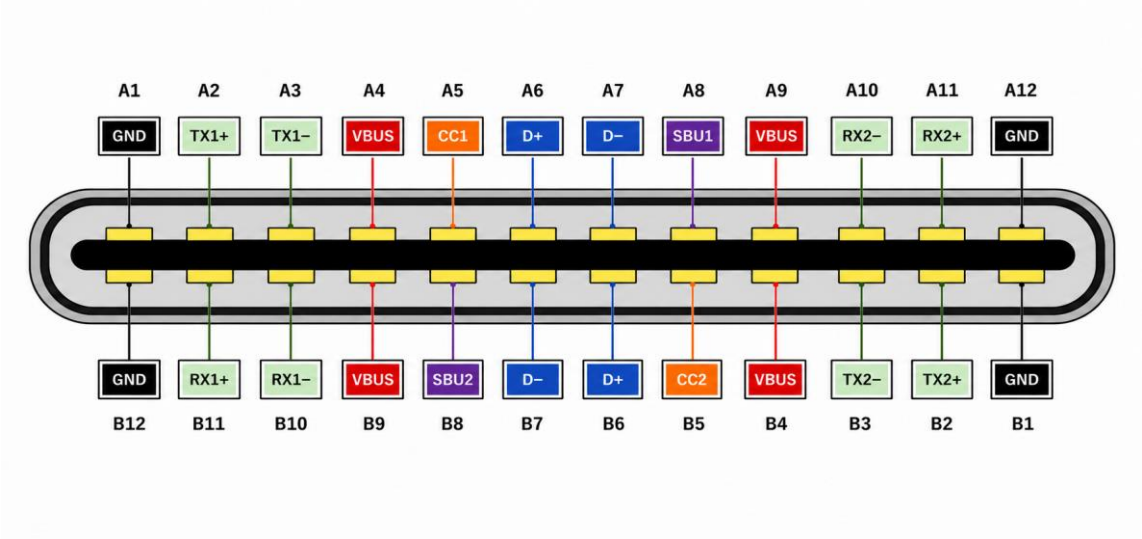

Figure 2.3: USB Type-C Connector Pin Diagram

In USB Type-C interfaces, the CC pins play an important role in enabling USB Power Delivery operation and cable orientation detection. During connection, the active CC line is selected automatically depending on the connector orientation, after which USB PD communication is established between the source and sink devices.

For electronically marked cables supporting higher current capability, the unused CC pin can provide a VCONN supply required for cable side circuitry operation.

VBUS pins carry VBUS power, while ground pins provide the return current path. The CC1 and CC2 pins are mainly used for cable orientation detection, source and sink identification, and USB Power Delivery communication. Figure 2.3 shows the USB Type-C pin connector pin names.

Depending on cable orientation, one CC pin becomes active for communication while the other may provide VCONN supply for electronically marked cables. Multiple VBUS and GND pins help distribute current and reduce connector resistance during high-power charging.

2.6 Configuration Channel (CC) Communication

The Configuration Channel (CC) pins form the primary communication interface in USB Type-C charging systems. Two CC pins, namely CC1 and CC2, are available in the connector for cable orientation detection, device attachment detection, and USB Power Delivery communication.

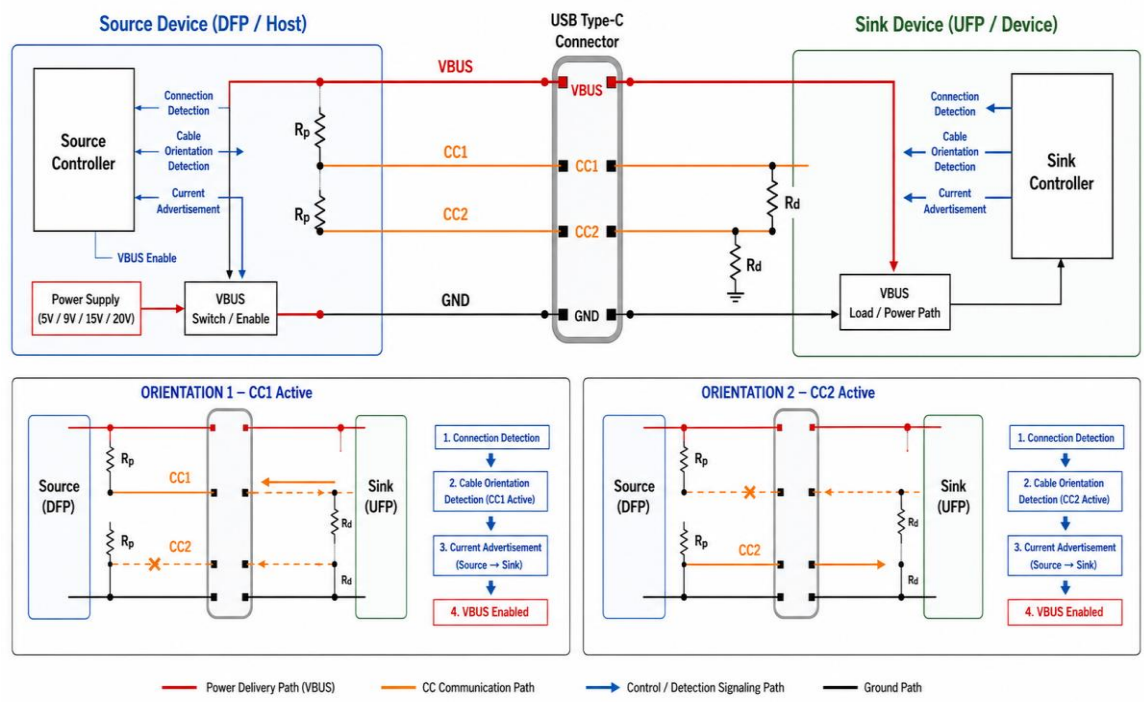

Figure 2.4: CC Communication and Connection Detection

Depending on cable orientation, either CC1 or CC2 becomes active for communication between the charger and the connected device. The source side has pull-up resistors (Rp), while the sink side uses pull-down resistors (Rd) as shown in Figure 2.4.

During USB PD operation, communication takes place over the active CC line using Biphase Mark Coding (BMC) signaling [7]. The sink device then requests the required power profile.

2.7 USB PD Voltage Profiles

USB PD supports multiple predefined voltage and current profiles called Power Data Objects (PDOs), allowing the charger and connected device to negotiate suitable operating conditions according to power requirements.

Unlike conventional fixed voltage USB charging systems, USB PD utilizes Configuration Channel (CC) communication for programmable power negotiation between source and sink devices.

During protocol negotiation, the source device advertises its supported PDO profiles, after which the sink device requests an appropriate voltage and current level according to device power requirements.

USB PD 3.1 introduced Extended Power Range (EPR) operation supporting voltage levels up to 48V. In addition to fixed PDO operation, USB PD also supports APDO-based PPS operation.

Table 2.5: USB PD voltages Profiles and Power Capability

USB PD Type	Voltage Profile	Max Current	Max Power	Applications
Standard Power Range (SPR)	5V	Up to 3A	15W	Smartphones, accessories
SPR	9V	Up to 3A	27W	Fast charging smartphones and tablets
SPR	12V	Up to 3A	36W	Tablets, portable devices
SPR	15V	Up to 3A	45W	Tablets
SPR	20V	Up to 3A	60W	Laptops, docking systems
SPR (E Marked Cable)	20V	Up to 5A	100W	High power laptops, monitors
Extended Power Range (EPR)	28V	Up to 5A	140W	Gaming laptops, workstations
EPR	36V	Up to 5A	180W	Industrial and power tools
EPR	48V	Up to 5A	240W	Automotive, high power systems

2.8 Programmable Power Supply (PPS)

PPS is a feature in USB Power Delivery that enables the charger to dynamically adjust its output voltage and current based on the device's charging needs.Table 2.6 compares fixed PDO and PPS operation and Table 2.7 displays the ranges of PPS and their application [22].

During charging, the sink device communicates with the source via the CC line using APDOS to exchange USB PD messages.

Table 2.6: Comparison of fixed PDO and PPS Operation

Parameter	Fixed PDO Operation	PPS Operation
Voltage Type	Fixed voltage levels	Dynamically adjustable voltage
Voltage Profiles	5V, 9V, 15V, 20V	3.3V–11V / 16V / 21V
Voltage Resolution	Fixed only	20 mV steps
Current Resolution	Fixed current	50 mA steps
Communication Type	PDO	APDO
Charging Efficiency	Moderate	High
Thermal Performance	Higher heat generation	Reduced thermal losses
DC-DC Conversion Loss	Higher	Lower
Battery Optimization	Limited	Improved
Typical Applications	Laptops, tablets	Fast charging smartphones

Table 2.7: Typical PPS Voltage Ranges and Application

PPS Voltage Range	Maximum Power Capability	Applications
3.3V – 11V	Up to 45W	Smartphones
3.3V – 16V	Up to 65W	Tablets, ultrabooks
3.3V – 21V	Up to 100W	High power USB PD devices

2.9 USB PD Communication and Negotiation

USB PD communication starts only after the cc line communication is built. After connection establishment, the charger shows the supported voltages and current profiles to the connected device so that it can accept according to its needs.

The sink which is on the phone side selects PDO based on its required voltage and current level. Once the request is accepted, a power contract is established and the charger transitions VBUS to the negotiated voltage level.

Communication between the charger and connected device takes place over the active CC line using Biphase Mark Coding (BMC) signaling. During charging, the connected device may periodically request different voltage or current levels depending on battery condition and power requirement.

2.10 DP/DM Based Charging Communication

Earlier fast charging standards such as QC, AFC, FCP, and BC1.2 relied on DP and DM signaling for charger detection and voltage selection. Different charging protocols use specific voltage signaling methods on DP and DM pins to identify charger capability and supported charging modes.

In BC1.2 operations, DP and DM lines are used for charger type detection and higher current operation indication. QC protocols also support voltage selection through predefined DP/DM voltage combinations for different charging profiles.

Many automotive USB charger ICs continue to support DP/DM based communication in addition to USB PD operation in order to maintain compatibility with legacy charging devices.

During practical testing, protocol analyzers such as Charger LAB power z can monitor supported charging protocols, negotiated voltage profiles, and charging behavior under different operating conditions. Voltages at DP/DM pins can also be seen by this device.

2.11 Conclusion

In this chapter, I reviewed the development of USB charging technologies from conventional 5V USB charging to modern USB Type-C Power Delivery systems. The older method of charging a smartphone works on 5V. Now the different protocols are getting into light that shows other voltage profiles.

In literature review we looked at how people have contributed to the development towards increasing the efficiency of the charger. Many problems are there in older methods that are being addressed and are removed.

In practical testing we found out that many innovations have been done towards the charger circuitry, protocol detection and how efficiently the charging can be done.

CHAPTER 3 - HARDWARE EXPERIMENTAL SETUP

3.1 Automotive USB PD Charging System Architecture

The whole idea of the experiment is that 48V will come from the battery that will come down to 12V by buck converter and based on the pins that are attached to the charger and the device the protocol will get activated that starts the charging of the connected device.The system was designed for electric two wheeler applications requiring compact mobile charging support as shown in fig 3.1.

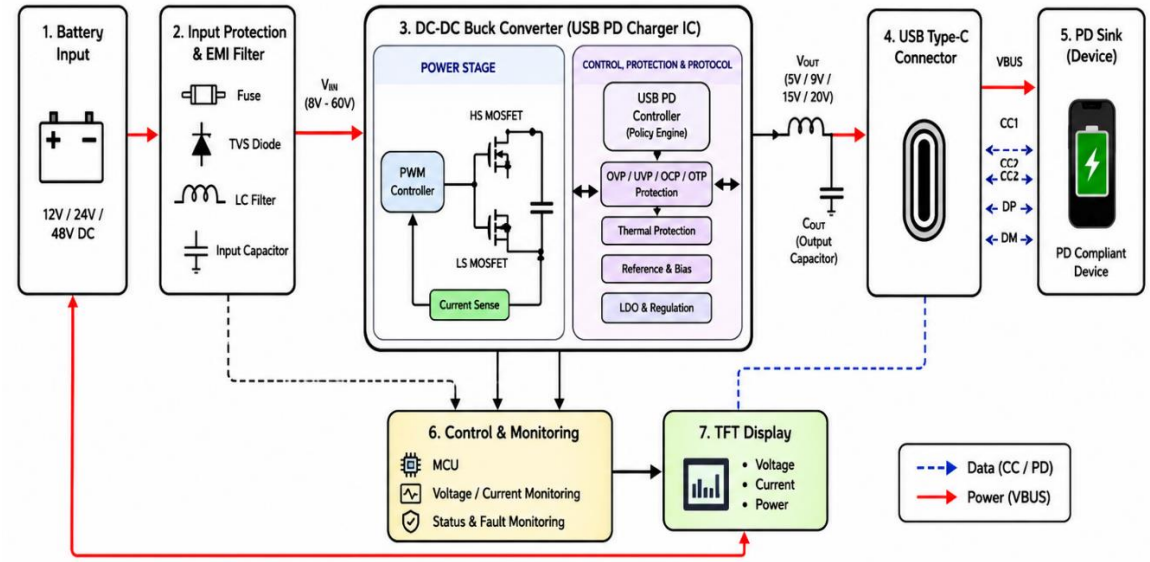

Figure 3.1: Overall architecture of the implemented USB PD charging system

Input power is drawn from the vehicle battery through an input filter and a protection stage with reverse polarity protection. These circuits maintain stable operation during voltage fluctuations and reduce noise.

The power conversion stage uses a synchronous buck converter integrated in the USB PD charger IC.

3.2 Injoinic IC Architecture and Operating Principle

The Injoinic IC is a synchronous buck converter that has USB Type-C Power Delivery chargers for fast charging. It operates within an input range of 7.3V to 29.5V and can be programmed to output up to 12V, delivering a maximum power of 36W [11].

Figure 3.2 shows the pin diagram of the Injoinic IC. This chip includes internal power MOSFETs, buck converter control, USB PD communication, current sensing, and protection features. It adjusts the output voltage according to the charging profile and load conditions[24].

The Injoinic IC works with several fast charging protocols, such as USB PD, PPS, QC, AFC, FCP, and BC1.2. USB PD uses the CC lines for communication, while older protocols use the DP and DM lines.

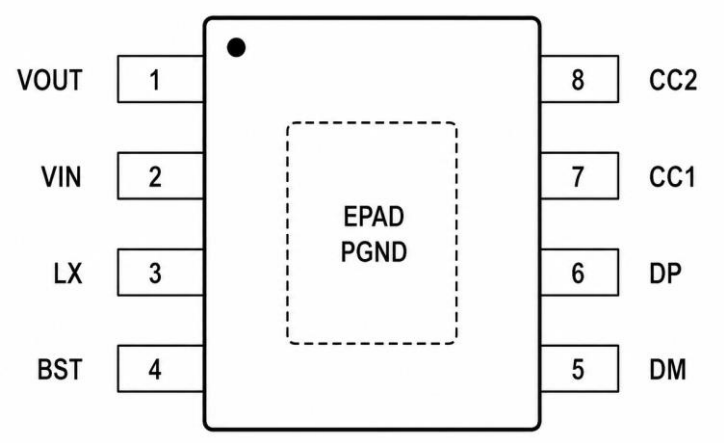

Figure 3.2: Pin Diagram of Injoinic IC

3.2.1 Injoinic IC Internal Architecture

The internal architecture consist of working of each pin and the main control block will get all the information about the vin,vout,lx pin. Figure 3.3 shows the functional block digram of the injoinic IC [24].

The IC has a syncronous buck converter stage, a USB PD communication controller, gate-driver circuitry, current-sensing blocks, feebback-control circuitry, and build in protection modules [11].

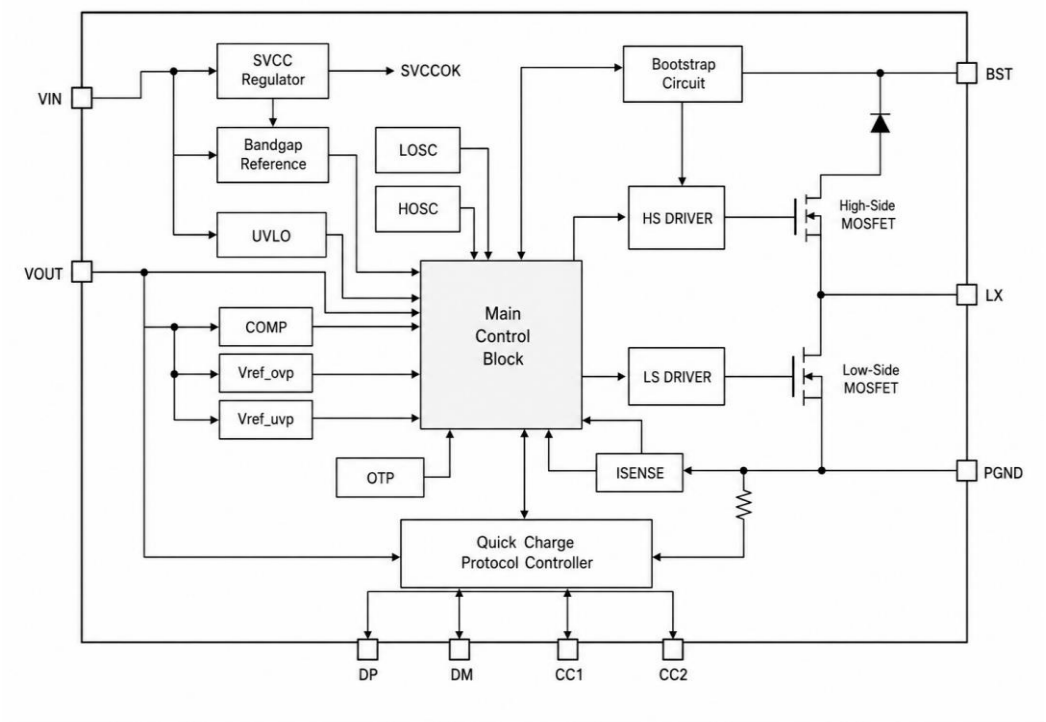

Figure 3.3: Functional Internal Architecture of Injoinic IC

3.2.2 Injoinic IC Functional Description

Figure 3.4 shows how the Injoinic IC based USB PD charger system works. The charger system gets its power from the scooter battery. This power is managed by the power stage to provide the correct voltage for the USB Type-C output.

The control and protection parts of the charger system handle communication with the USB PD, manage the voltage, and ensure the charger system charges safely.

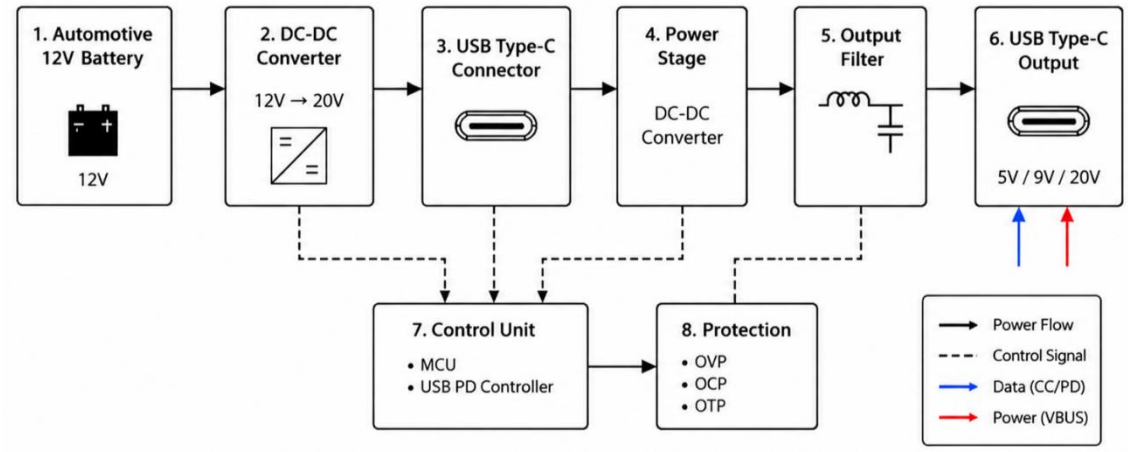

Figure 3.4: Functional flow diagram of Injoinic IC

3.2.3 Schematic Design of Injoinic IC Based USB PD Charger

The output stage features external inductors and filter capacitors positioned close to the switching node to decrease output ripple and enhance stability. RC snubber networks, made of 390pF capacitors and 2Ω resistors, are connected near the LX switching node to minimise voltage ringing and overshoot caused by high-frequency switching.

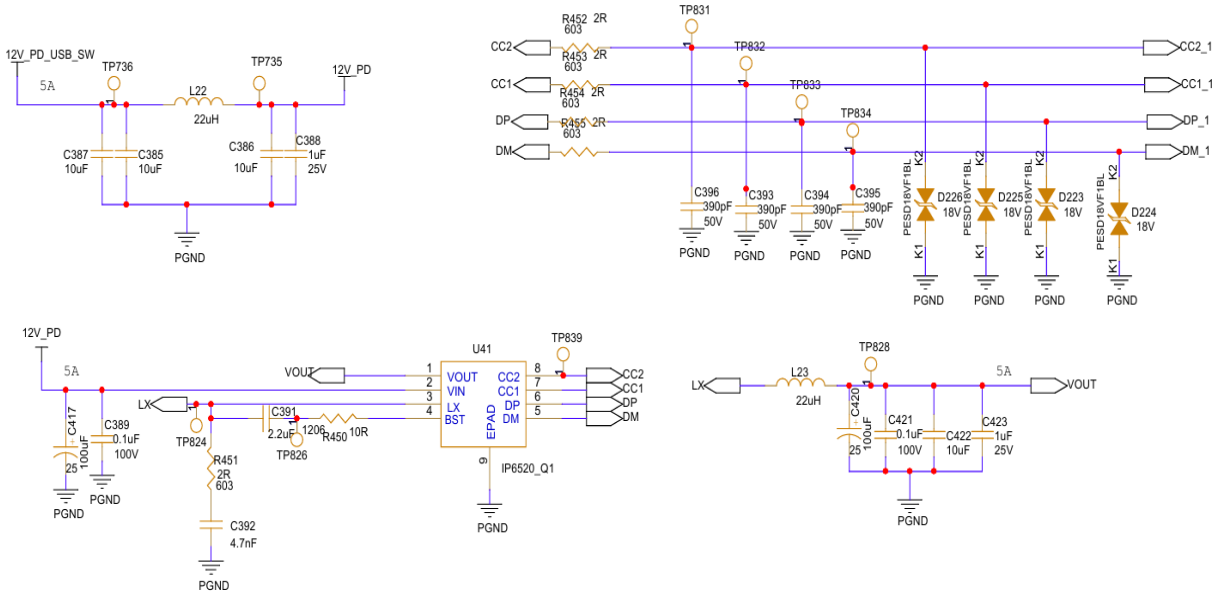

Figure 3.5: Injoinic IC Schematic Designed in Cadence

The LX pin shows the switching waveform when connected to a DSO. The output stage features external inductors and filter capacitors positioned close to the switching node to decrease output ripple and enhance stability.

RC snubber networks, made of 390pF capacitors and 2Ω resistors, are connected near the LX switching node to minimise voltage ringing and overshoot caused by high-frequency switching.

ESD protection devices were connected across the CC1, CC2, DP, and DM communication lines using protection diodes to remove voltage or current spikes.

3.2.4 Input Power Stage Design

The input power stage is designed for fluctuating battery voltage caused by load changes, switching transients, and disturbances. It features bulk capacitors, EMI filters, reverse polarity protection, and transient suppression. Figure 3.6 shows the placement of capacitors and an inductor that filter the 12V input.

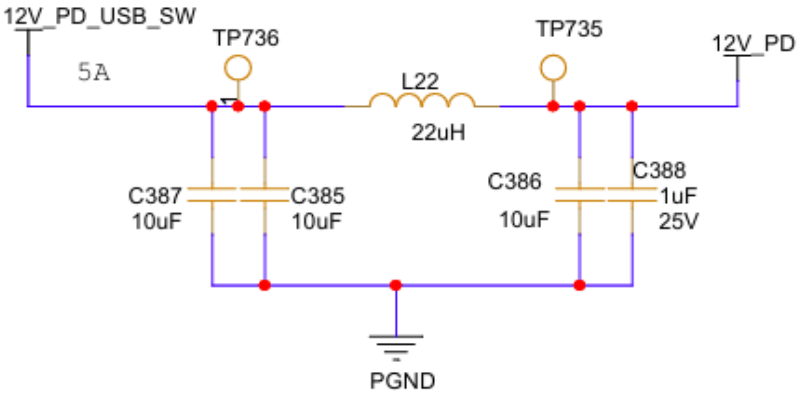

Figure 3.6: Injoinic IC Input LC Filter and Protection Circuit

3.2.5 Buck Converter Power Stage

The Injoinic IC's power conversion stage employs a synchronous buck converter design to transform automotive input voltage into stabilised USB PD output levels. It features internal high-side and low-side MOSFET switches, complemented by external inductors and output filter capacitors.

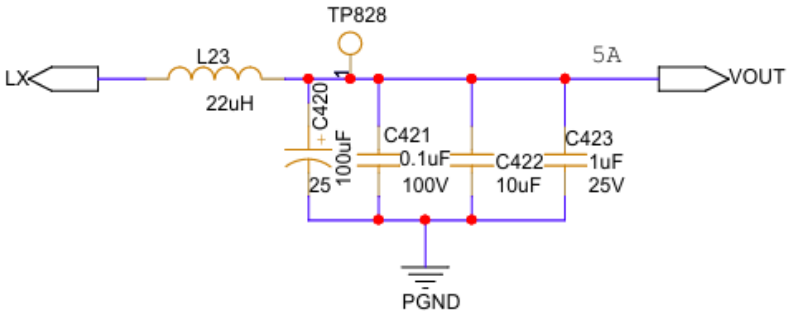

Figure 3.7: Injoinic IC Buck Converter Power Stage

The VIN pin draws input power from the automotive supply through filtering and protection circuitry. The SW node links to the external inductor and output filter stage for efficient power conversion and regulation.

A bootstrap capacitor connects between the BST and SW pins to facilitate high-side gate drive operation.

The regulated VBUS output is produced after the inductor and output capacitor stage connected to the switching node. The FB pin monitors the output voltage via the feedback network to ensure a stable output under changing load conditions and various USB PD profiles.

3.2.6 Output Configuration and Passive Component Design

Output voltage regulation is managed via the feedback network connected to the FB pin, which monitors VBUS output to ensure stable operation across various USB PD voltage profiles.

The output voltage configuration depends on an external feedback resistor divider connected between VBUS, the FB pin, and ground. Figure 3.8 illustrates the passive components of the Injoinic IC in the schematic.

The chosen inductor value was based on switching frequency, ripple current, and load conditions. Selecting the inductor influences ripple current, transient response, and the overall stability of the converter during operation.

Input and output capacitors were selected considering voltage rating, ripple handling capability, and stability requirements during converter operation.

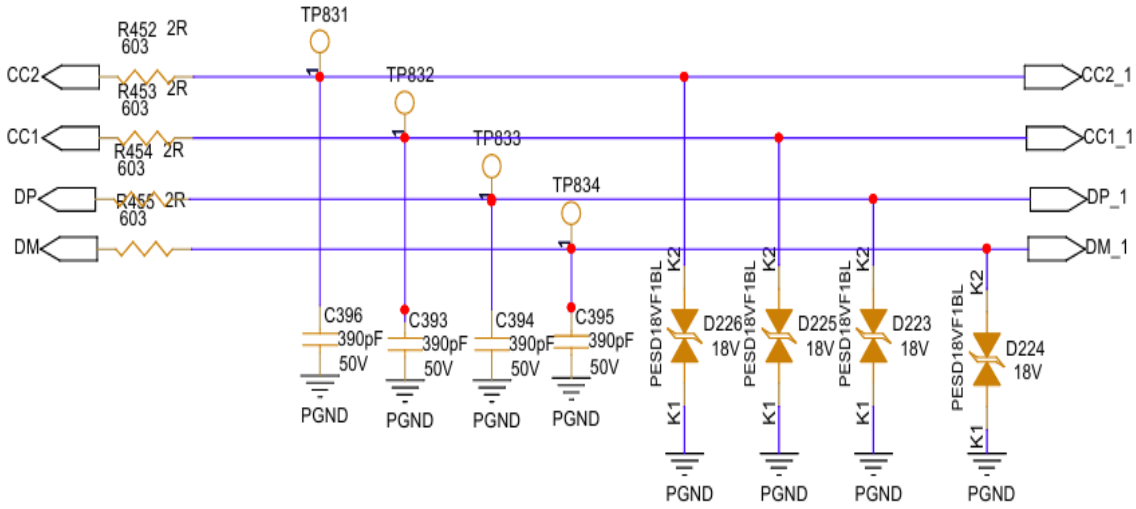

Figure 3.8: Injoinic IC Passive Component Placement in Schematic

3.2.7 TFT Display Board Integration

The TFT board image has a connector which pin are connected to the IC through PCB wires and we have taken capacitors and inductor, and the protection circuitry based on the specifications mentioned in the documents. Figure 3.9 the compact TFT enabled the implementation of the scooter USB Type C charging interface within the vehicle dashboard system.

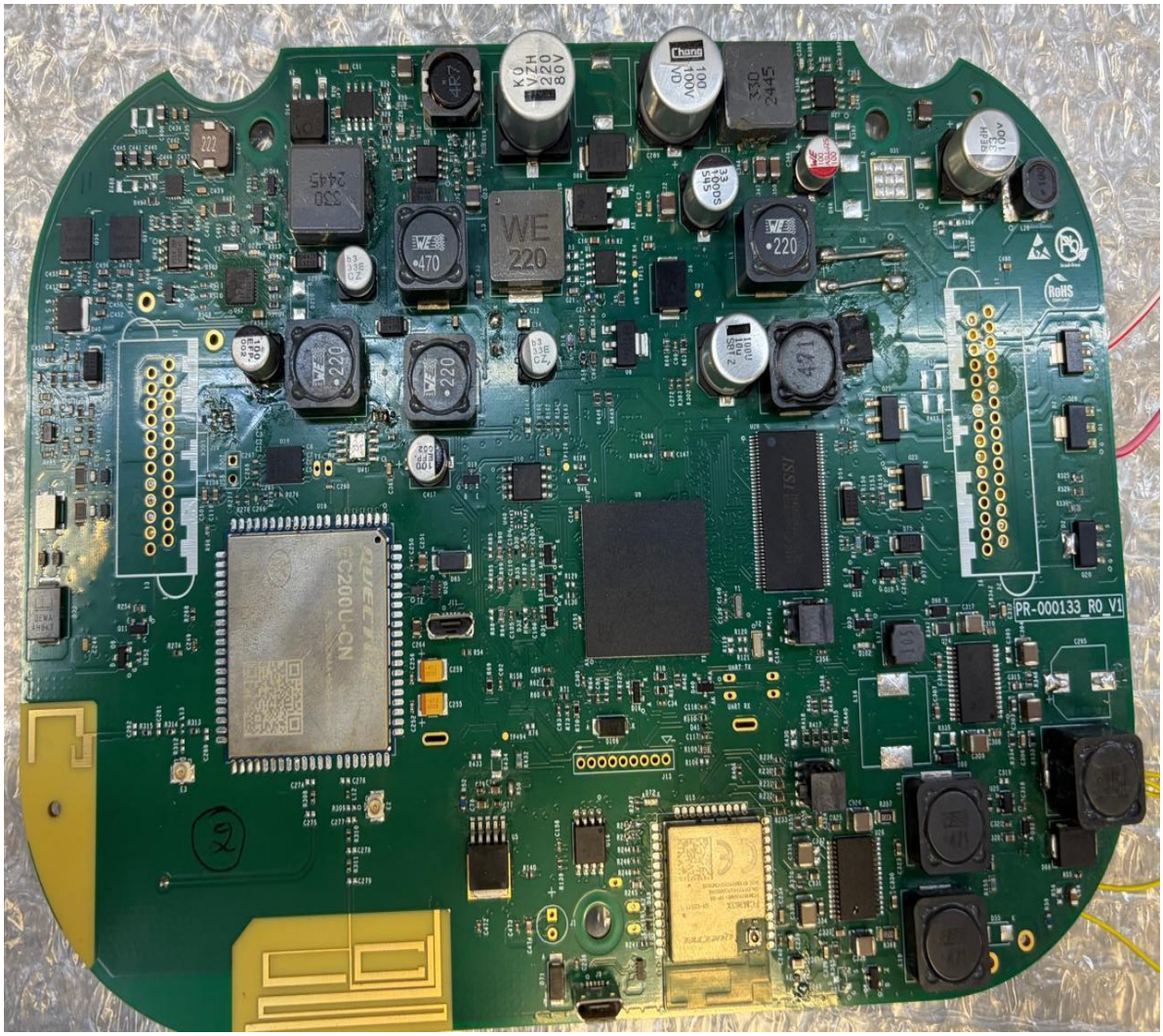

Figure 3.9: 5-Inch TFT Display Control Board with Injoinic IC

3.3 MPS Evaluation Board Architecture

The MPQ4241, developed by Monolithic Power Systems (MPS), is an USB Type-C Power Delivery solution designed for vehicle applications. It combines a synchronous buck converter integrated power MOSFETs, protocol detection circuitry, and protection features in a compact package.

Figures 3.10 and 3.11 display the front and rear sides of the MPS. The device operates within an input voltage range of 4.5V to 24V and provides output voltage settings from 3.3V to 21V, capable of delivering up to 65W of power.

The IC can be programmed for voltages PDO or APDO, it depends on the client that wants to access the devices based on the required changes.

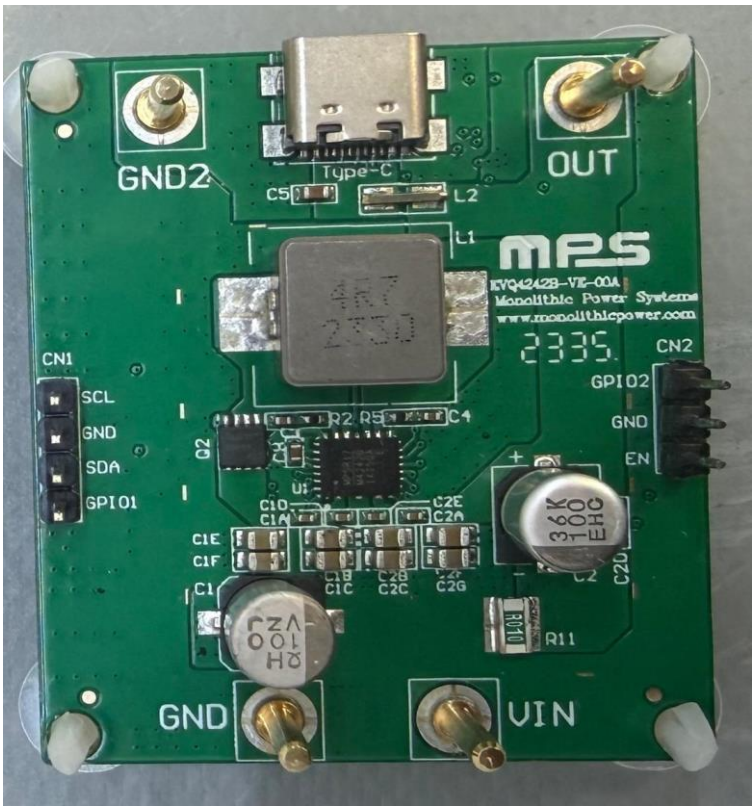

Figure 3.10: Front side of MPS Evaluation Board

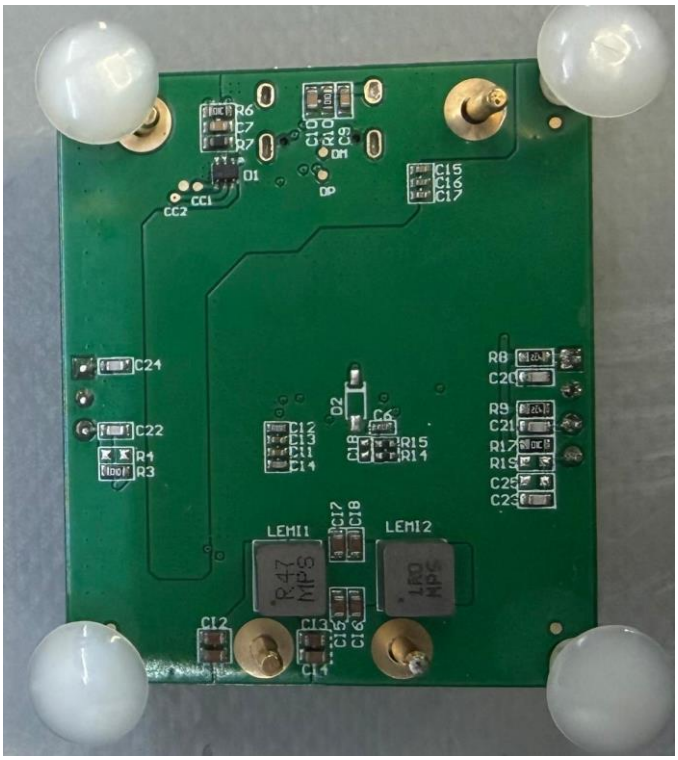

Figure 3.11: Rear side of MPS Evaluation Board

3.3.1 MPS Internal Architecture

The MPS is a compact USB Type-C Power Delivery controller for high-efficiency fast charging in automotive and industrial systems, combining a buck converter, communication controller, gate drivers, protection, and protocol functions.

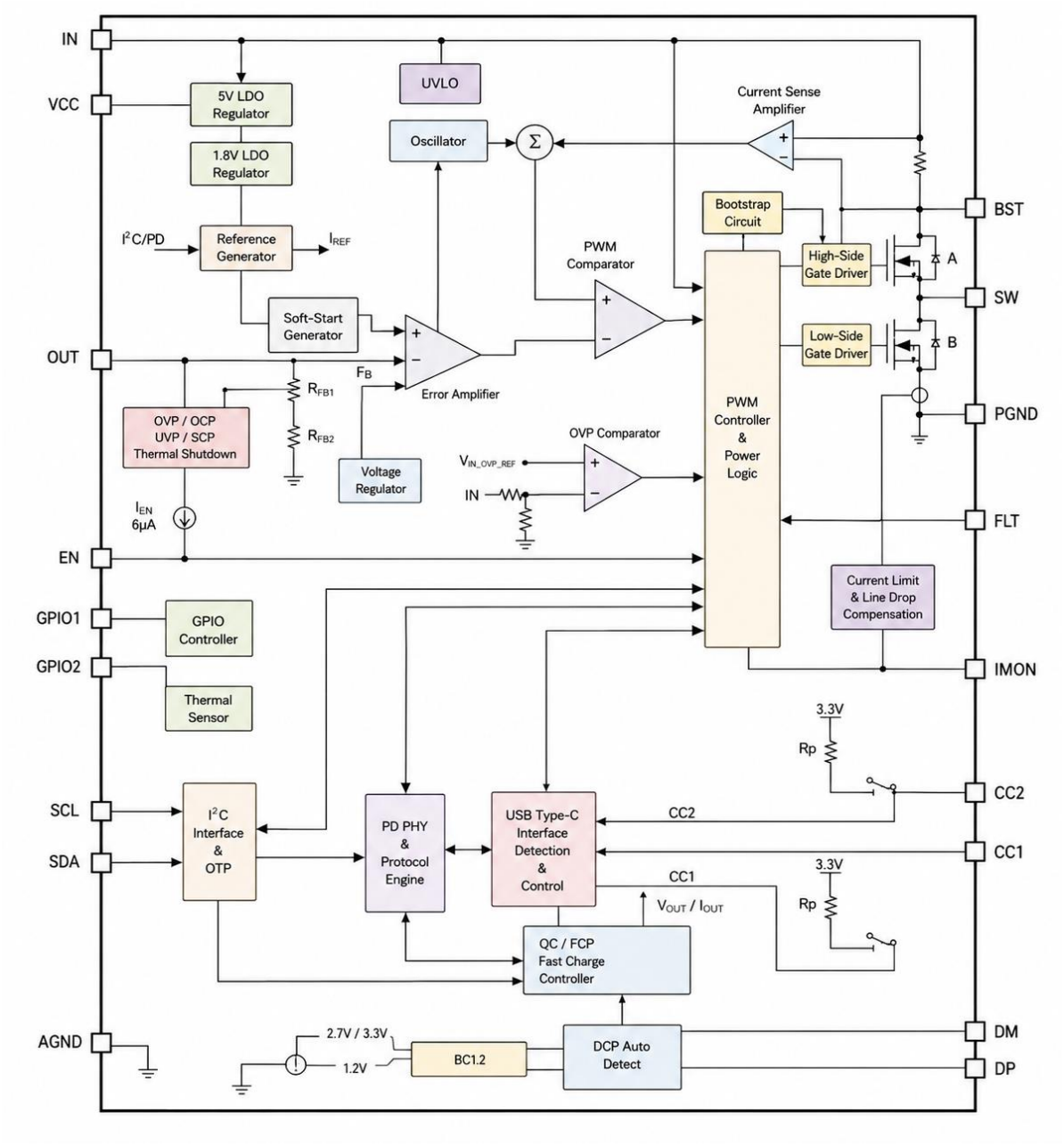

Figure 3.12: Internal Functional Architecture of MPS Evaluation Board

The controller supports wide input voltage operation and programmable USB PD output profiles for Type-C charging applications.

The internal power stage uses a synchronous buck converter with integrated high and low-side MOSFETS. The IN pins supply voltage to the converter and control circuits.

The SW node connects to an external inductor for energy transfer and regulation. A bootstrap capacitor on the BST pin enables high-side gate drive. Figure 3.12 shows the MPS evaluation board's internal architecture.

Output voltage regulation is controlled by the internal feedback and PWM circuitry according to the negotiated USB PD profile and load conditions. The integrated low RDS(ON) MOSFET structure helps reduce switching and conduction losses during high-current operation.

The MPQ4241's communication section features CC1 and CC2 interfaces for USB Type-C attachment detection and USB PD signaling. It also includes DP and DM interfaces to support legacy charging protocols like QC, BC1.2, and FCP. Additionally, the controller supports I2C communication via SDA and SCL pins, enabling configuration of parameters such as PDO profiles, protection settings, switching frequency, and line compensatio

Additional GPIO features are included for external monitoring and control, such as thermal sensing, fault indication, and LED operation.

3.3.2 Functional Description of MPS

The schematic of MPS board is given below in figure 3.13, the IC is conned to capacitors in input to filter the input voltage and the inductor stores the charger when the mosfets are not active and complete the loop.

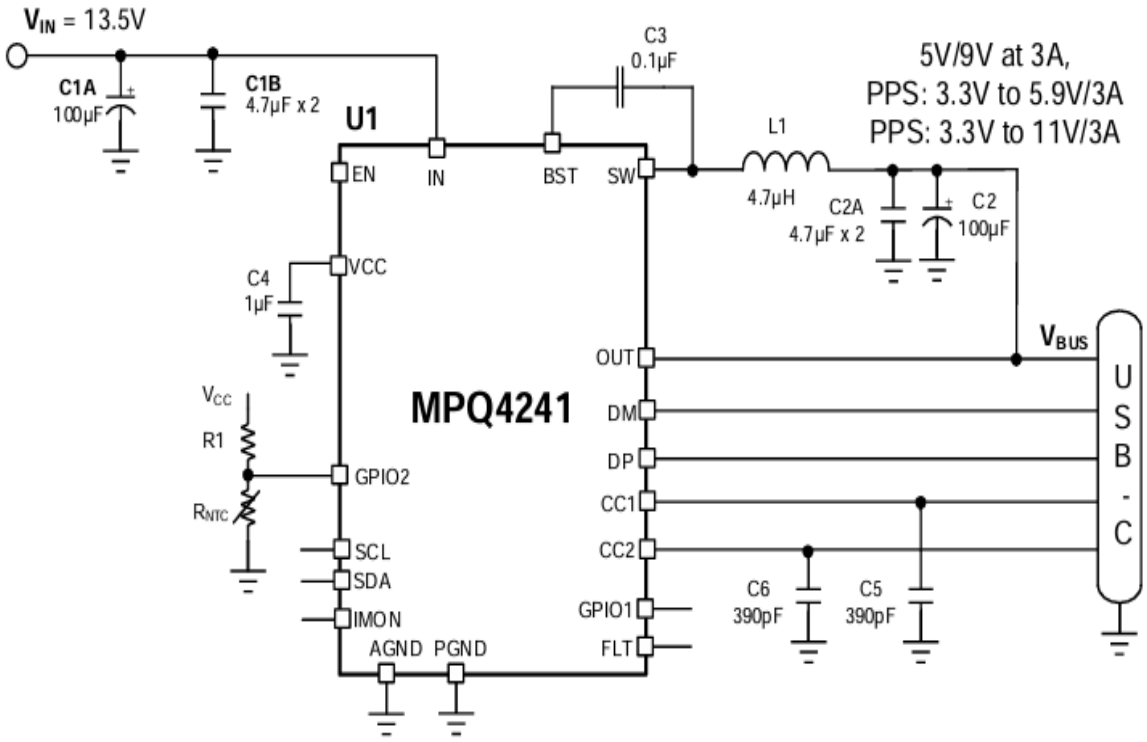

Figure 3.13: Application Circuit of MPQ4241 USB PD Controller

3.3.3 Virtual Bench Pro Configuration

The MPQ4241 evaluation board was set up. We took a look at it using Monolithic Power Systems Virtual Bench Pro software. This software talked to the computer through the USB to I2C interface on the MPS Evaluation Board. This lets us get to the settings of the MPQ4241 IC controller.

We set up the PDO profiles using the interface so they would work for our tests. This is shown in figure 3.15, which shows what the Virtual Bench Pro interface looks like when we use it to set up the MPS.

The Virtual Bench Pro software kept an eye on the voltage and the status of the converter. It also watched for problems. Checked the temperature.

The interface on the computer screen allowed us to watch what was happening with the protection events, like when there was too much current, when it was getting too hot, and when the voltage was too low [12].

When we were testing, we needed to make sure the connections were correct and that the digital control registers on the MPQ4241 were set up properly so that the communication between the devices would work smoothly.

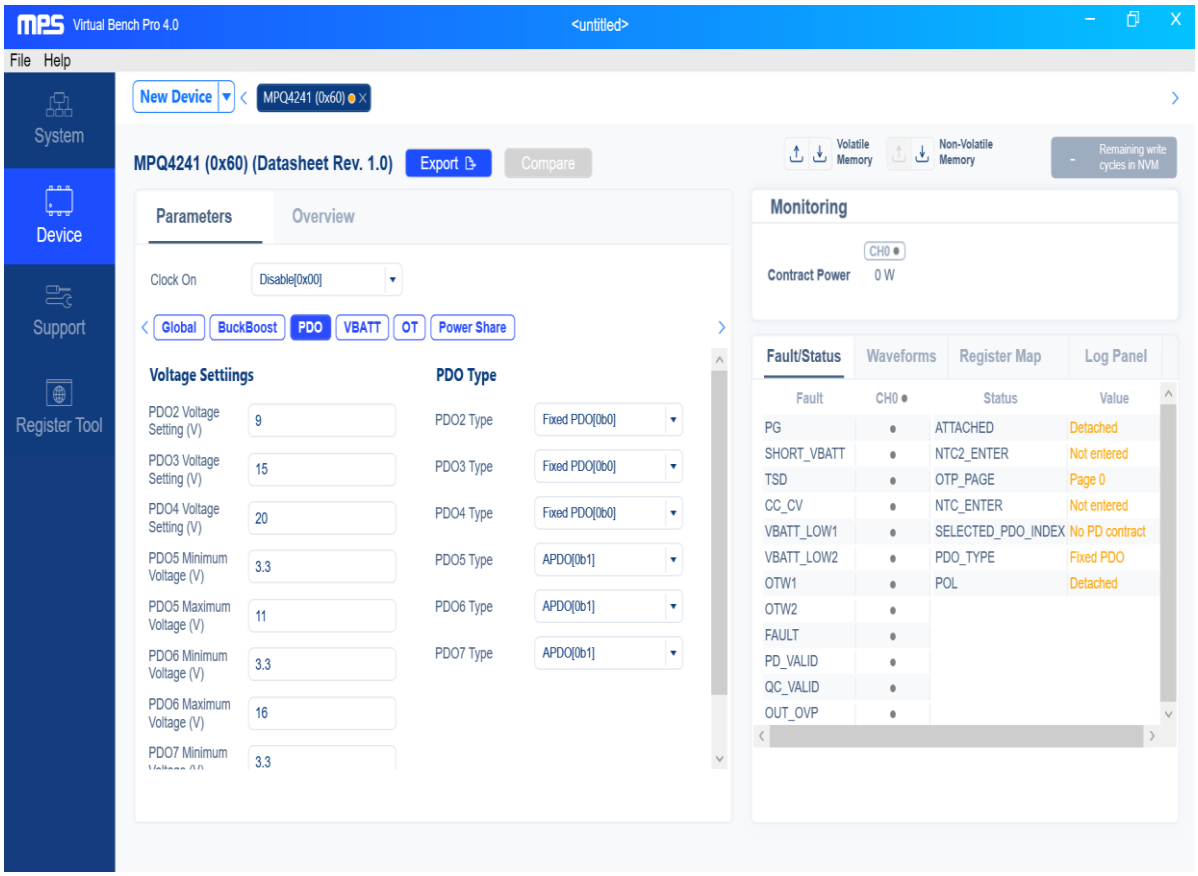

Figure 3.14: Virtual Bench Pro Interface Used for MPS Configuration

3.4 Renesas Evaluation board

The Renesas evaluation board is made for high power USB PD applications. These applications need the board to be very efficient and work well with input voltages [13].

The Renesas evaluation board uses a 3-level synchronous buck architecture. This architecture helps to reduce energy losses when the board is switching. It also reduces the stress on the power MOSFETs when the board is working with power [26].

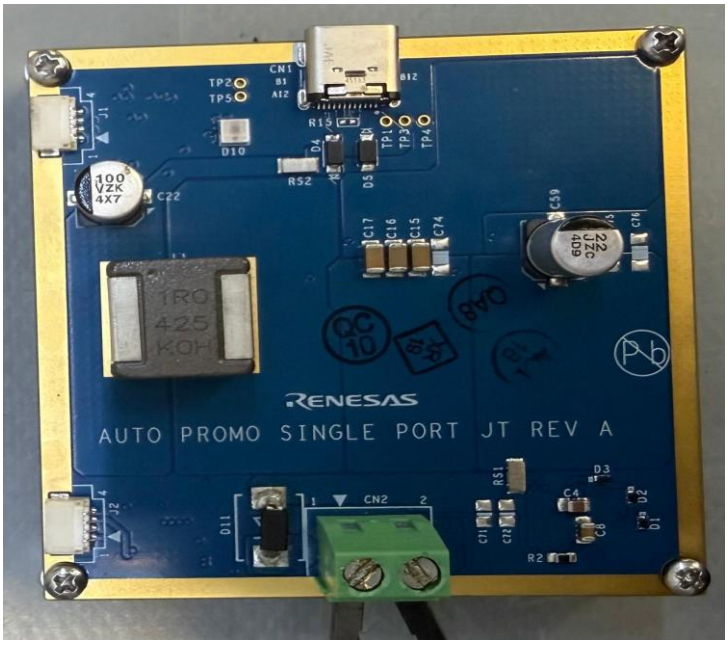

Figure 3.15: Front view of Renesas Evaluation Board

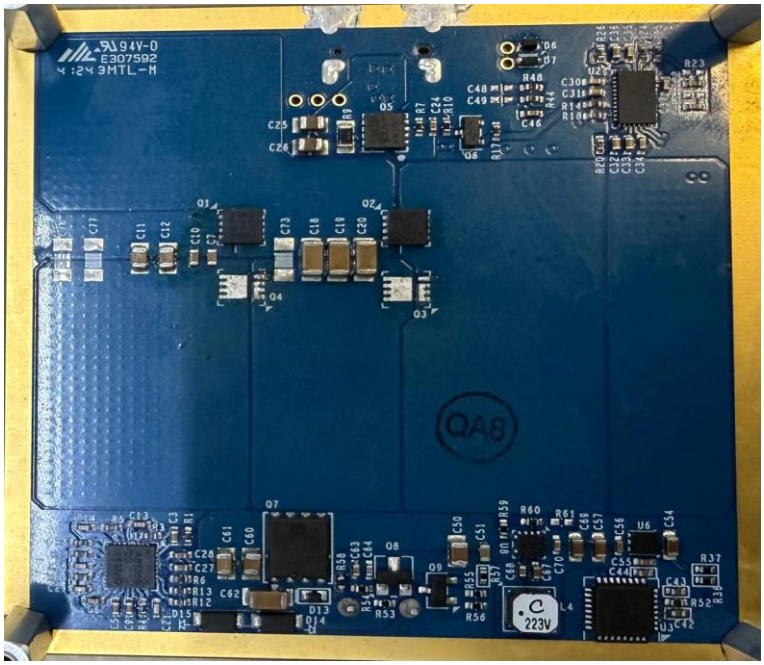

Figure 3.16: Rear view of Renesas Evaluation Board

The 3-level switching architecture enhances efficiency during high current operation and enables smooth transitions between CCM and DCM modes based on load. Protection and monitoring features ensure reliable operation during USB PD power delivery.

.3.4.1 3-Level Buck Converter Architecture

The Renesas Board uses a 3-level buck converter for high-power USB PD up to 140W. Unlike a 2-level converter, it reduces voltage stress on MOSFETs by using a flying-capacitor topology, cutting switching losses and boosting efficiency at high frequency [14].

The microcontroller controls MOSFETs via gate-driver circuitry. When the USB is attached, it signals the IC to open the circuit and pass power from the IC to the USB-C. Its flying capacitor network ensures stable voltage at switching nodes. The architecture supports lower inductance and improved switching behavior at the output [27].

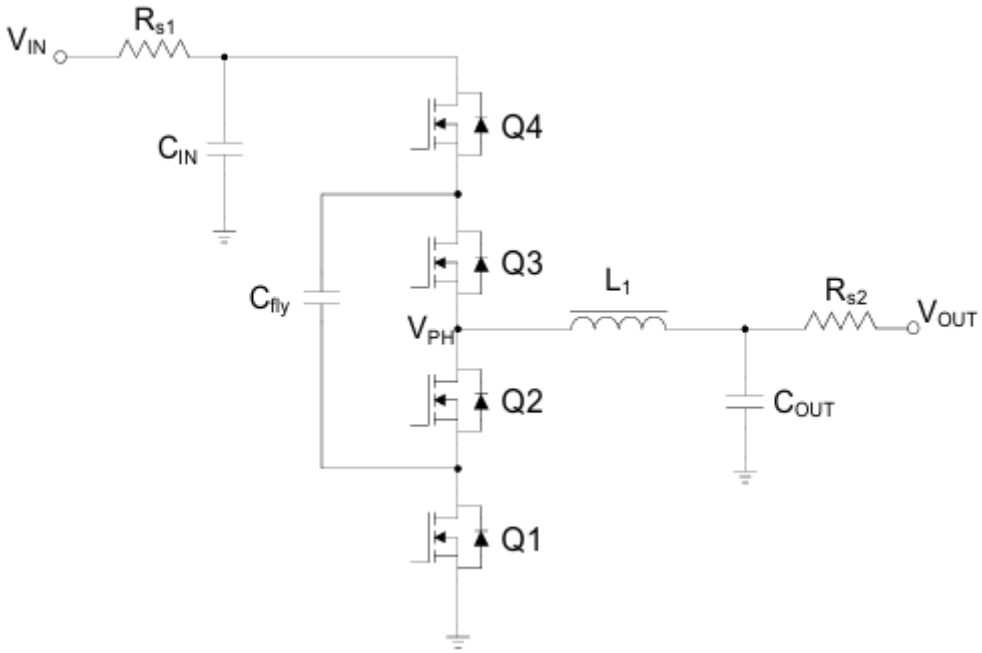

Figure 3.17: 3-Level Buck Converter Topology

The evaluation board works on 48V automotive batteries and delivers USB PD outputs up to 28V/5A. It switches MOSFETs based on the duty cycle to achieve higher efficiency at high voltages. With over 98% efficiency at high loads, it reduces thermal stress, ideal for high-power automotive charging.

3.4.2 Renesas Board USB Type-C Port Controller

The RAA489400 functions as the USB Type-C Port Controller within the Renesas USB PD. The controller is responsible for USB Type-C attachment detection, CC communication, VCONN management, and USB PD protocol handling during charging.

The device supports USB PD 3.1 communication and Extended Power Range operation for high-power USB Type-C applications.

Figure 3.19 shows the Renesas board's internal architecture, including VBUS monitoring, Fast Role Swap and dead battery support.

The RAA489400 also integrates protection functions for VBUS, CC lines, and VCONN operation to improve reliability during USB PD operation.

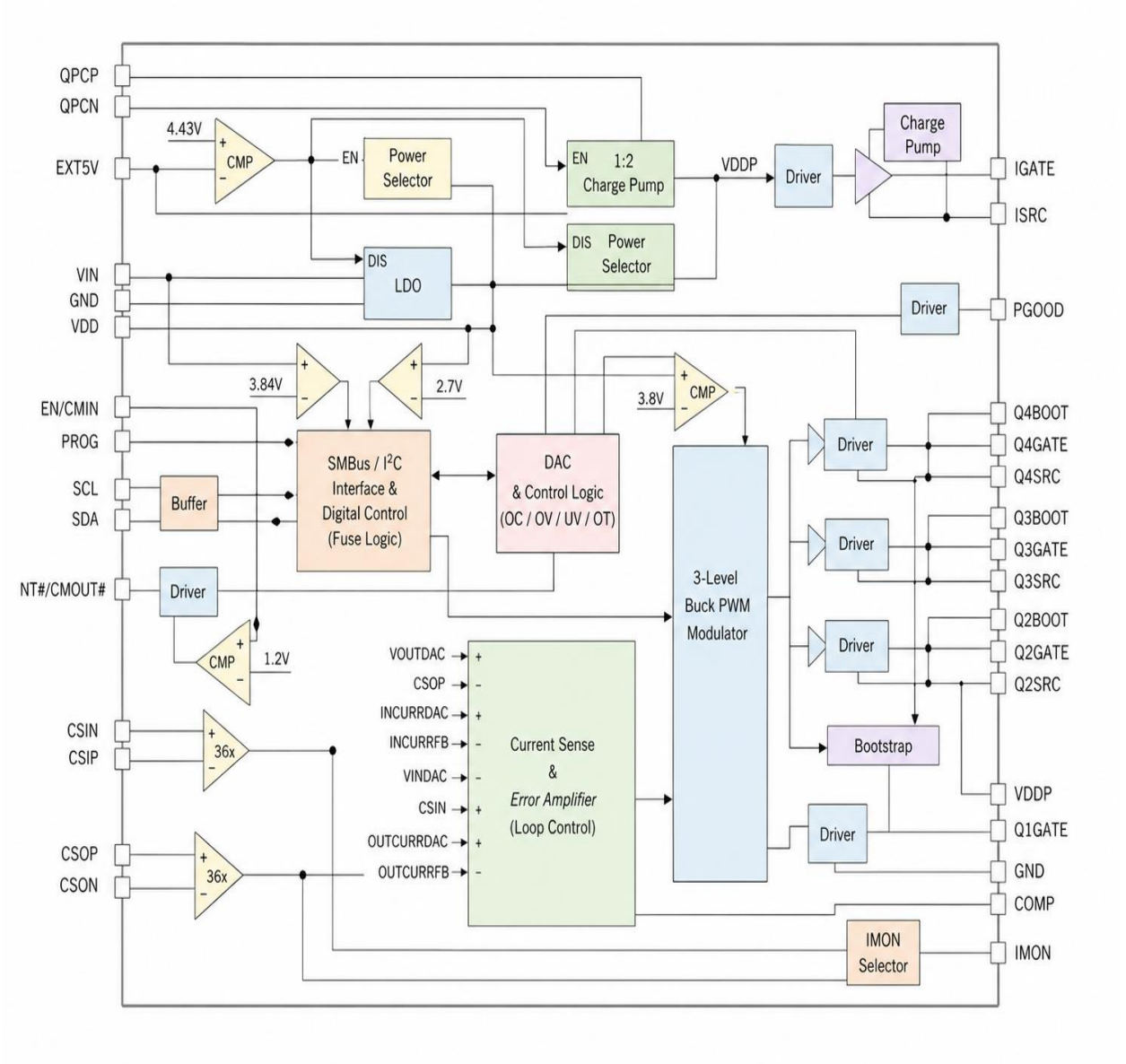

Figure 3.18: Renesas Board Internal Functional Architecture

3.5 Comparative Hardware Analysis of Selected Charger ICs

The evaluated USB PD charging s utilize different power conversion architectures and protocol management approaches depending on target power level and automotive application requirement. Table 3.2 summarizes the major hardware characteristics and electrical specifications of the selected charger.

Table 3.2: Hardware Comparison of Selected USB PD Charger ICs

Parameter	**Injoinic IC**	**MPS Board**	**Renesas Board**
Converter Topology	Synchronous Buck	Synchronous Buck	3-Level Buck
Input Voltage Range	7.3V – 29.5V	4.5V – 24V	4.5V – 57.6V
Max Input Voltage	36V	36V	60V
Output Voltage Range	3V – 12V	3.3V – 21V	3V – 54.9V
Max Output Power	36W	65W	140W
Max PDO Profile	9V/3A	20V/3.25A	28V/5A
USB PD Version	PD2.0 / PD3.1	PD3.1	PD3.1 EPR
PPS Voltage Range	3V – 11V	3.3V – 11V	Up to 48V
PPS Resolution	20mV	20mV	Software Configurable
Suorted Charging Protocols	QC2.0, QC3.0, AFC, FCP, SCP, BC1.2	QC4+, BC1.2, Apple Divider, FCP	USB PD 3.1 EPR
MOSFET Configuration	Integrated	Integrated	External MOSFET Stage
High-Side MOSFET RDS(ON)	Internal	30mΩ	External
Low-Side MOSFET RDS(ON)	Internal	18mΩ	External
Switching Frequency	Internal PWM Control	250kHz / 420kHz / 2.2MHz	Up to 400kHz
Peak Efficiency	93.27%	98.22%	Approximately 98%
Thermal Derating	Internal OTP	Starts at 130°C	Programmable
Thermal Shutdown	Internal OTP	170°C	Supported
Target Application	Compact Automotive USB Charging	Mid Power Fast Charging	High Power Automotive Charging

3.6 Conclusion

This chapter delineated the hardware design and implementation of the selected automotive USB PD charging s. The Injoinic IC charger was successfully integrated onto the TFT display board with appropriate filtering, protection, and USB Type-C communication circuitry.

The MPS MPQ4241 offered enhanced configurability and support for advanced USB PD features, including PPS operation and programmable PDO profiles. The Renesas board exhibited support for higher power USB PD operation through its three-level buck converter architecture [12].

Overall, the chapter gave a clear look about each of the IC that are being used, describes each stages, pins and the software that has been used.

CHAPTER 4 - EXPERIMENTAL ANALYSIS

4.1 Experimental Test Setup

The experimental setup utilised for the performance assessment of the USB Type-C Power Delivery s is depicted in Figure 4.1. Testing was conducted employing a programmable DC power supply, a PD sink module, and an electronic DC load to evaluate efficiency, load regulation, and protection behavior under various operating conditions. The input power was supplied via the DC power supply, whereas the output load current was regulated using the electronic load.

During MPS evaluation testing, the board was connected directly to the PD sink module using USB Type-C. When using the Injoinic IC on the 5-inch TFT board, a converter PCB was used between the TFT and the PD sink to enable USB-C conversion.

Different PDO voltage profiles and load currents were tested, with output monitored via oscilloscopes and lab instruments. Figure 4.1 depicts the USB PD performance hardware setup.

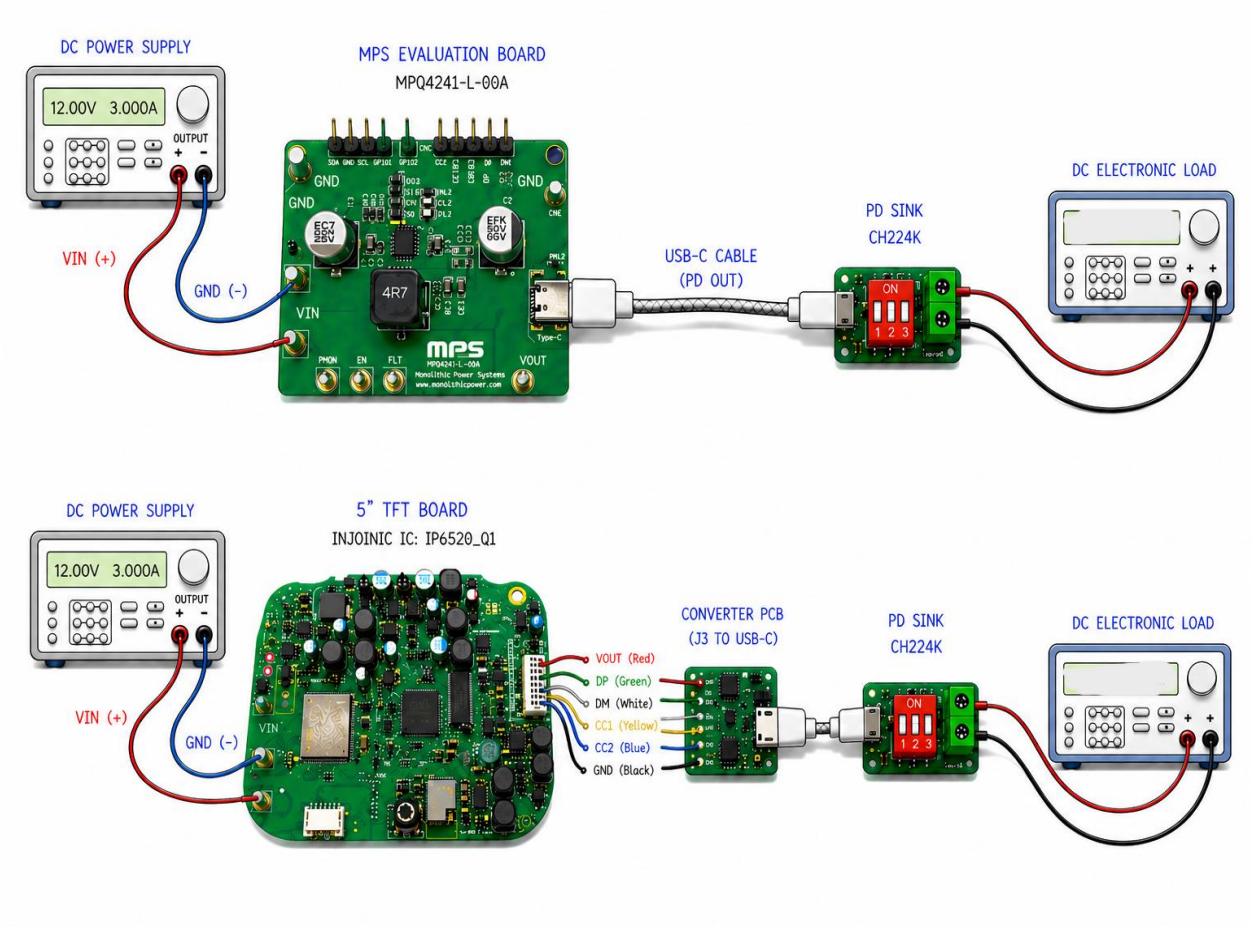

Figure 4.1: Hardware Setup for USB PD Performance Evaluation

4.1.1 Overall Hardware Test Bench

The experimental validation of the selected USB Type-C Power Delivery charger ICs used a hardware test bench with a programmable DC power supply, electronic load, oscilloscope, multimeter, USB PD sink trigger board, and Charger LAB protocol analyzer.

The input voltage ranged from 7.3v to 48v, depending on the charger architecture, to analyze converter behavior under low, nominal, and high voltage conditions. An electronic DC load in constant current mode evaluated load regulation and efficiency at different loads.

By configuring the sink selection pins, fixed PDO profiles ranging from 5V to 20v, including 9V, 12V, and 15V, were selected during testing.

The Charger LAB KM003C analyzer was interfaced between the charger output and the sink device to monitor the USB PD protocol negotiation, output voltage, current, power delivery status, and permissible charging protocols.

Oscilloscope measurements were performed during protection testing and transient analysis for observing converter startup behavior, output voltage recovery, hiccup operation, and protection triggering response.

4.1.2 USB PD Sink Trigger Board Configuration

The CH224K USB PD sink trigger module shown in FIGURE 4.2 and 4.3 was used in experiments to request different USB Power Delivery voltage profiles from the charger under test. It functions as a USB PD sink device, communicating with the charger via the CC lines of the USB Type-C interface.

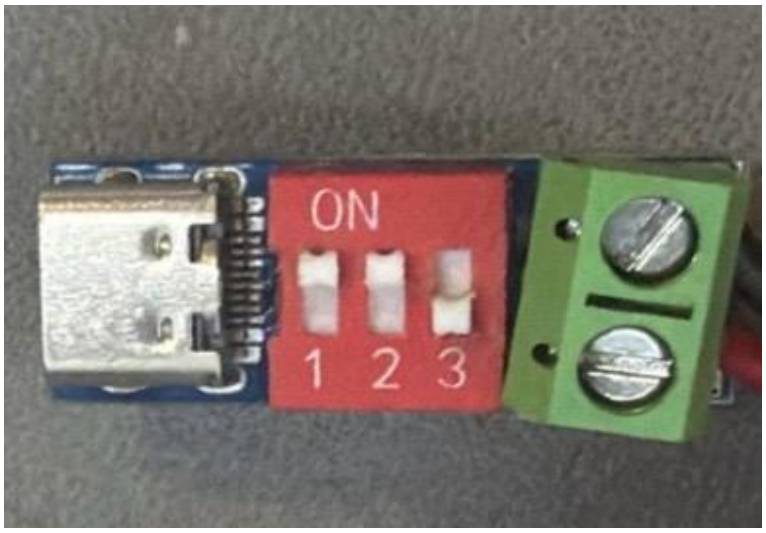

Figure 4.2: Front view of USB PD sink trigger module

Figure 4.3: Rear view of USB PD sink trigger module

The implemented CH224K sink board included DIP switch based voltage selection for requesting different PDO profiles including 5V, 9V, 12V, 15V, and 20V according to the configuration truth table shown in Table 4.1. During testing, the required voltage profile was selected manually through the DIP switch configuration before connecting the module output to the electronic DC load.

After successful USB PD negotiation, the selected output voltage became available at the output terminals of the module. The output was connected directly to the electronic DC load operating in constant current mode for load testing, efficiency measurement, and protection validation of the USB PD chargers.

The CH224K module was extensively used during testing of the INJOINIC IC, MPQ4241, and Renesas RAA489300 IC for verifying PDO negotiation, output stability, and USB PD communication behavior under different load conditions.

Table 4.1: CH224K PD Trigger Voltage Selection Table

SW3	SW2	SW1	Output Voltage
1	X	X	5V
0	0	0	9V
0	0	1	12V
0	1	1	15V
0	1	0	20V

4.1.3 Charger LAB Protocol Analyzer Setup

The Charger LAB KM003C USB PD analyzer was used during experimental validation for monitoring USB Power Delivery negotiation, output voltage, output current, charging power, and protocol behavior of the charger s under test. The analyzer was connected

between the USB PD charger output and the CH224K sink trigger module in order to observe real time charging parameters during operation.

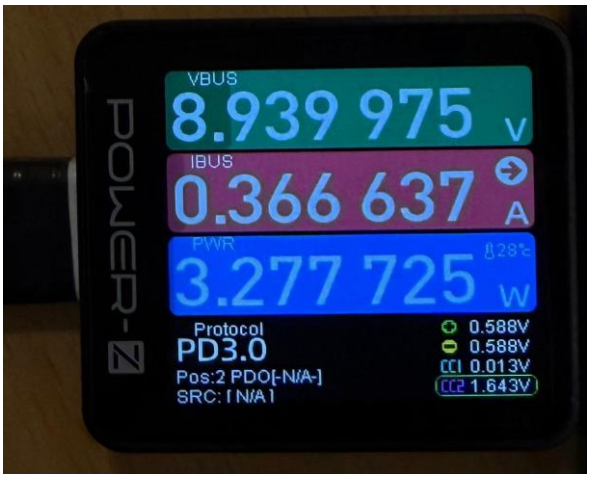

Figure 4.4: PD analyzer USB PD Output Monitoring

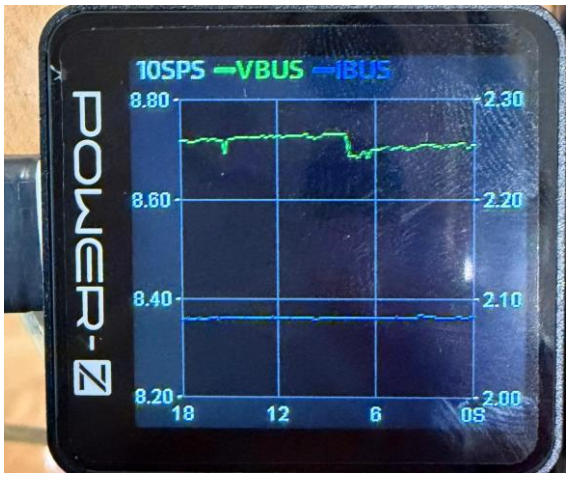

Figure 4.5: PD analyzer VBUS and IBUS Monitoring

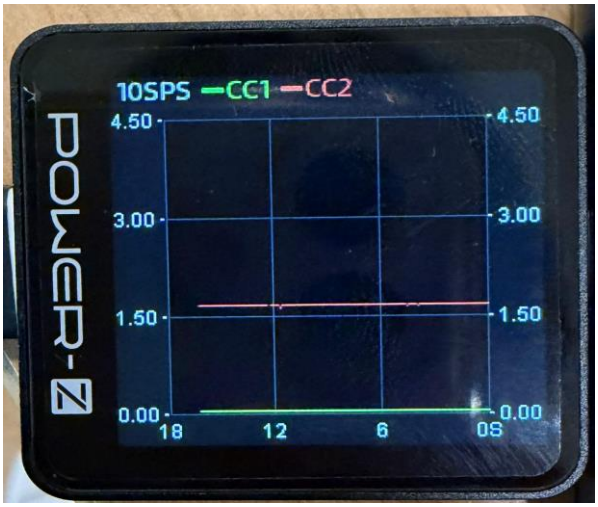

Figure 4.6: PD analyzer CC Line Monitoring

The analyzer provided monitoring of VBUS voltage, output current, output power, CC communication line voltage, negotiated PDO profile, and supported charging protocol during converter testing. During experimental evaluation, the KM003C was used for verifying successful USB PD negotiation under different operating conditions including 5V, 9V, PPS, and higher power load conditions.

The captured waveforms were used for observing voltage stability, current variation, and protocol behavior during load regulation testing.

The analyzer was also used for monitoring output behavior under different power levels during testing of the INJOINIC IC, MPQ4241, and Renesas RAA489300 charging s. Experimental observations obtained through the analyzer assisted in validation of PDO negotiation, PPS operation, and charging stability during load variation and high power testing conditions.

4.2 USB PD Voltage Profile Configuration

The Injoinic IC based USB PD charger was validated under different USB Power Delivery voltage profiles using the CH224K sink trigger module and Charger LAB KM003C analyzer. Different PDO profiles were selected through the DIP switch configuration before USB PD negotiation.

After successful Type-C attachment detection, the charger advertised the supported PDO profiles through the CC communication line.

The negotiated output voltage was verified using the KM003C analyzer and digital multimeter before load testing. As shown in Figure 4.7 stable PPS operation was observed near 15W load condition during experimental testing. Output voltage and charging current remained stable during continuous operation.

Figure 4.7: PD analyzer PPS Output Monitoring (15W)

During lower load testing, stable PPS negotiation and output regulation were also observed, as shown in Figure 4.8. Minor variation in output current was observed due to load change conditions

Higher power testing was additionally performed near 20W operating condition. Figure 4.9 shows stable USB PD operation with proper voltage negotiation and power delivery behavior during load testing.

Experimental observations showed stable voltage regulation under different operating conditions. Higher output current during lower voltage operation increased conduction losses within the converter power stage.

Figure 4.8: PD analyzer PPS Output Monitoring (12W)

Figure 4.9: PD analyzer USB PD Monitoring (20W)

4.3 Experimental Evaluation of Injoinic IC

Experimental testing of the Injoinic IC automotive USB PD charger was carried out under different input voltage and load conditions to evaluate converter efficiency and output regulation performance.

Initial validation was performed using the 27W charger configuration, followed by testing of the upgraded 36W hardware after modification of the converter stage and passive components.

Efficiency was measured at 5V, 9V, and 12V USB PD using a programmable power supply and electronic load.

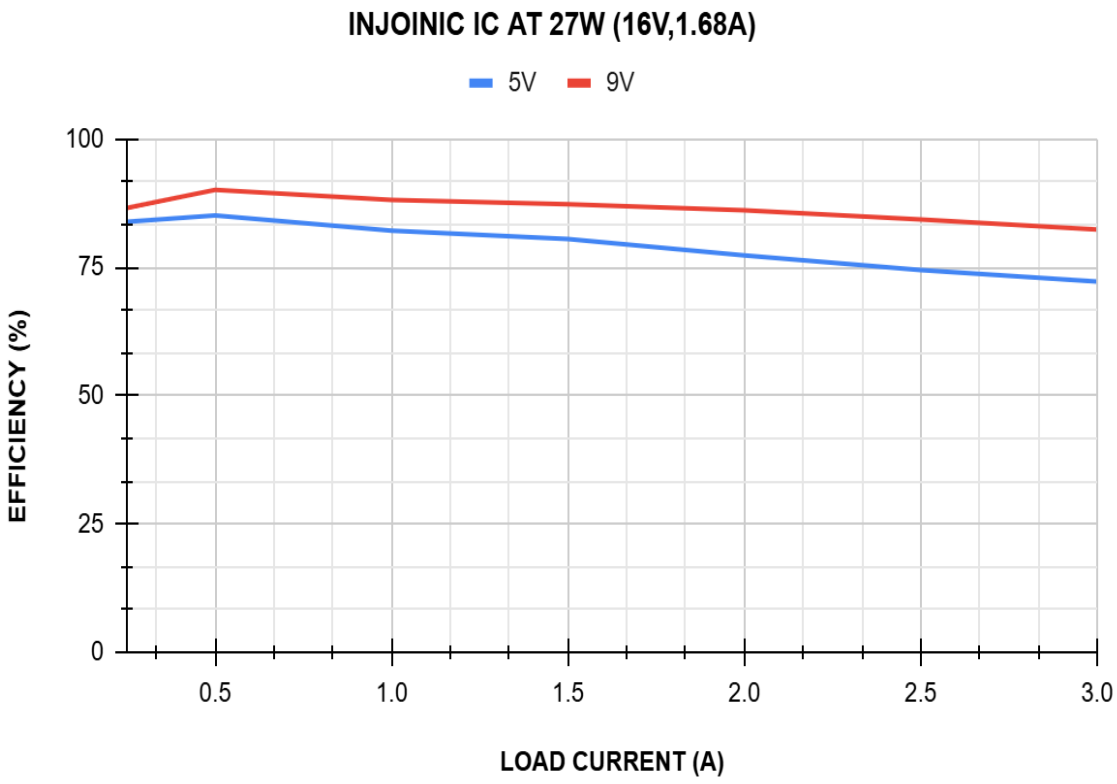

Figure 4.10: Injoinic IC Efficiency at 27 W and 16 V Vin

Efficiency variation of the 27W INJOINIC IC charger under 5V and 9V USB PD operation at vin at 16V. Maximum efficiency of 85.1% at 5V and 90.07% at 9V was observed near 0.5A load current. A gradual reduction in efficiency was observed under higher load-current conditions

Efficiency analysis was performed at Vin at 29.3V under 5V and 9V USB PD operation. Maximum efficiency of 83.6% at 5V was observed at 0.5A load current, while 9V operation achieved 85.6% efficiency at 1A load current.

.

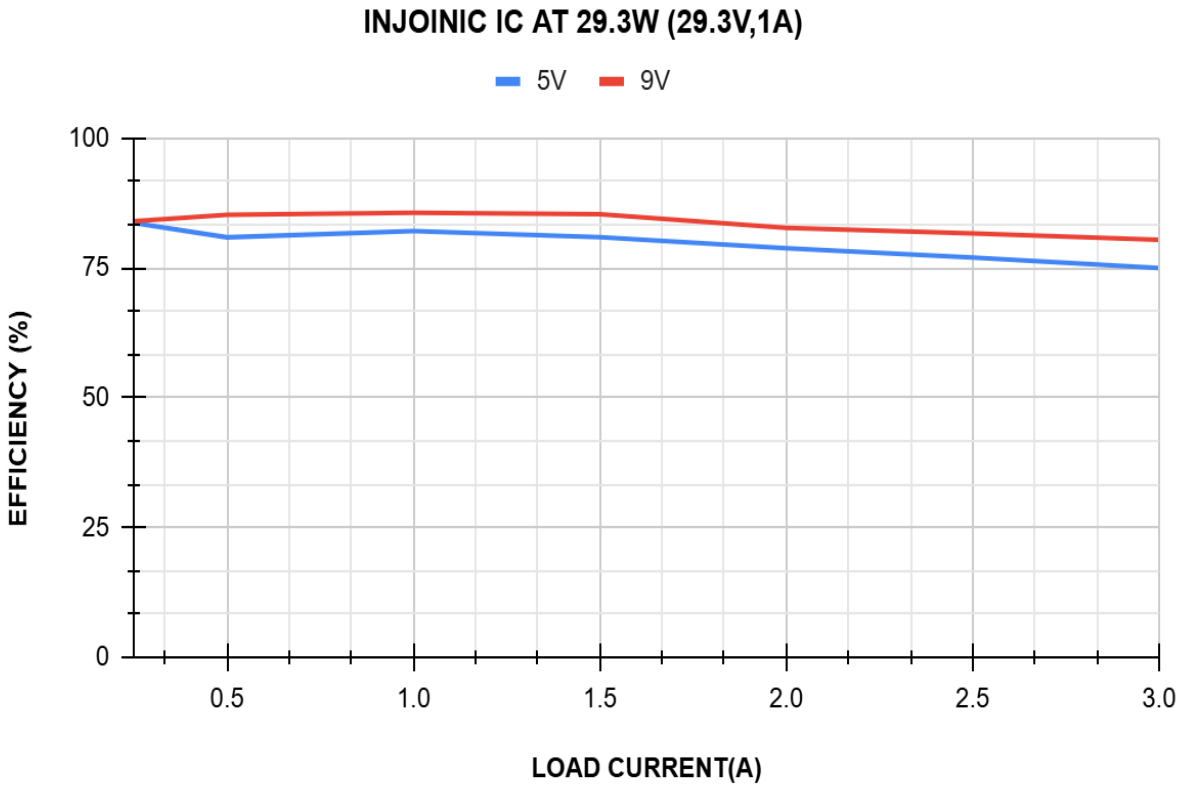

Figure 4.11: Injoinic IC Efficiency at 27W and 29.3V Vin

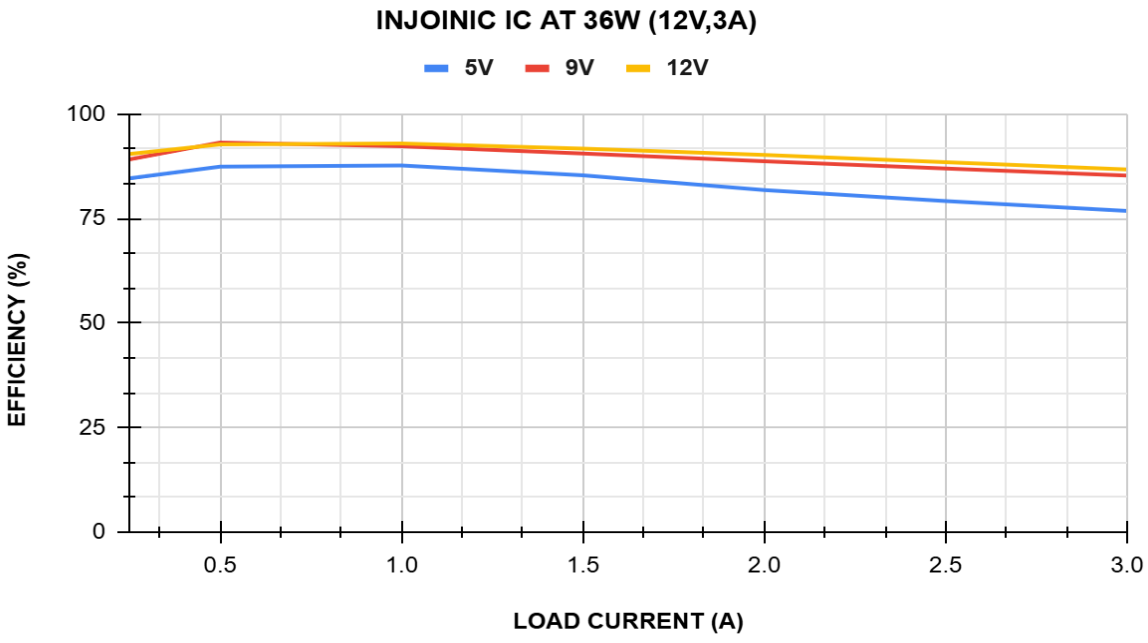

Figure 4.12: Injoinic IC Efficiency at 36W and 12V Vin

Figure 4.12 shows the efficiency performance of the upgraded 36W Injoinic IC charger under 5V, 9V, and 12V USB PD operation at 12V vin.
Maximum efficiencies of 87.6% at 5V, 93.2% at 9V, and 92.9% at 12V were observed during experimental testing.

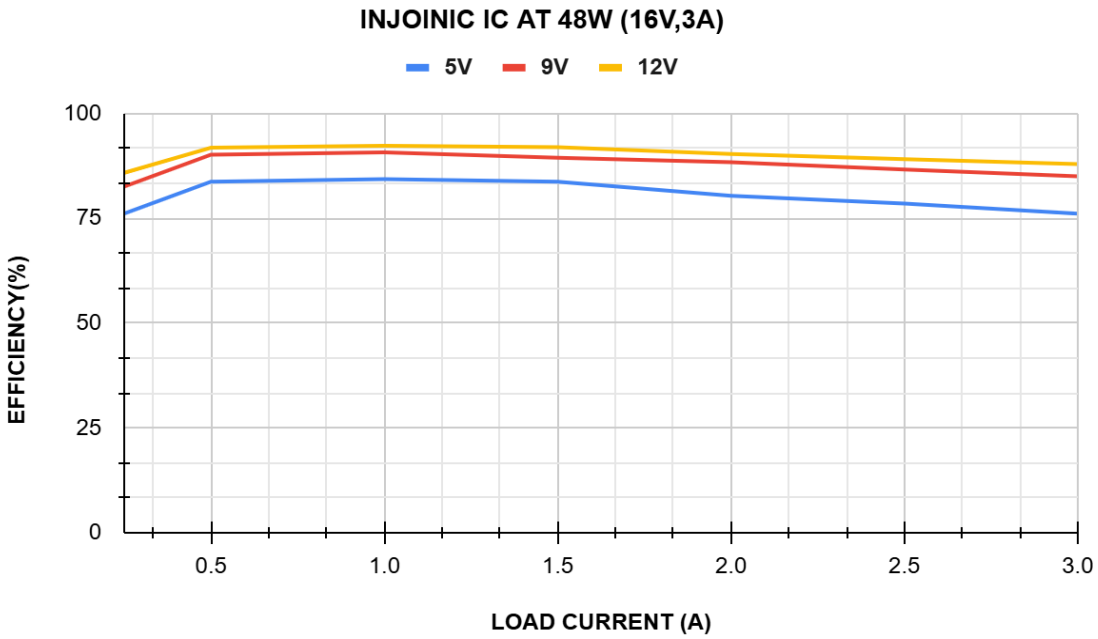

Figure 4.13: Injoinic IC Efficiency at 48W and 16V Vin

Efficiency analysis of the Injoinic IC charger was performed at VIN = 16V and 3A under 5V, 9V, and 12V USB PD operation.
Maximum efficiency of 84.3% at 5V, 90.7% at 9V, and 92.2% at 12V was observed at 1A load current.

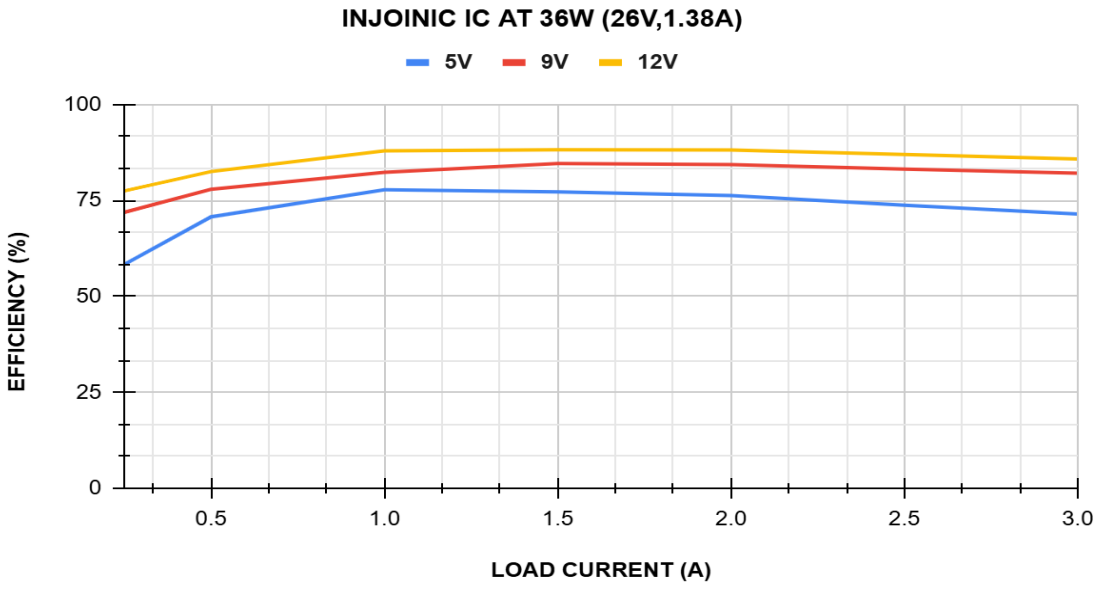

Figure 4.14: Injoinic IC Efficiency at 36W and 26V Vin

Efficiency analysis was performed at VIN at 26V and 1.38A under 5V, 9V, and 12V USB PD operation.
Maximum efficiency of 77.78% at 5V was observed at 1A load current, while 9V and 12V operation achieved 84.61% and 88.22% efficiency respectively at 1.5A load current.

4.4 Load Regulation Testing for Injoinic

Load regulation testing of the Injoinic IC charger was performed under different USB PD operating conditions by gradually increasing the electronic load current from 0.25A to 3A. Output voltage variation was monitored during 5V, 9V, and 12V USB PD operation to analyze converter stability under changing load conditions.

Figure 4.15 and Figure 4.16 show the load regulation characteristics of the initial 27W hardware configuration under 5V and 9V operation. A small reduction in output voltage was observed with increasing load current due to converter conduction and wiring losses.

After upgrading the hardware to the 36W configuration, improved output stability was observed under higher load conditions. Figure 4.17 and Figure 4.19 show stable load regulation during 5V, 9V, and 12V USB PD operation with lower voltage variation across the load range.

High-power testing was also conducted at elevated input voltage conditions. As illustrated in Figure 4.18 Hardware modifications, including the use of shorter wires, parallel inductors, low DCR inductors, and supplementary output capacitors, were empirically assessed under different USB Power Delivery (PD) operating conditions.

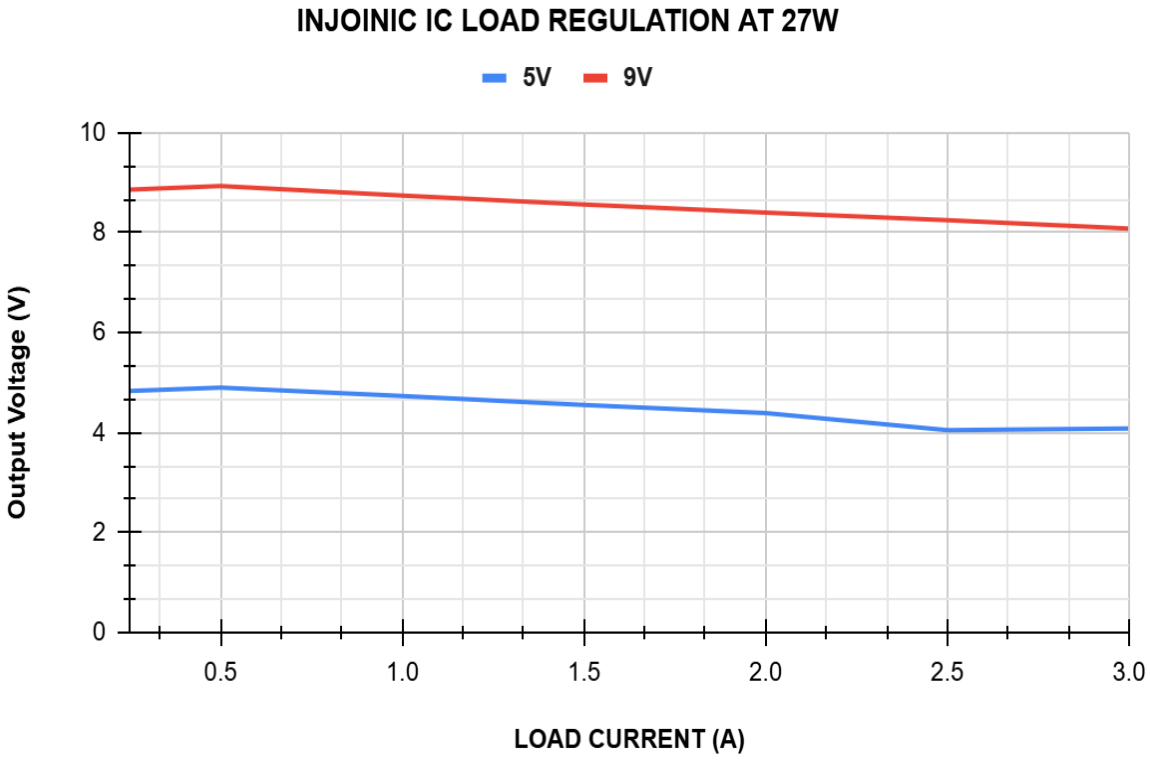

Figure 4.15: Injoinic Load Regulation at 27W

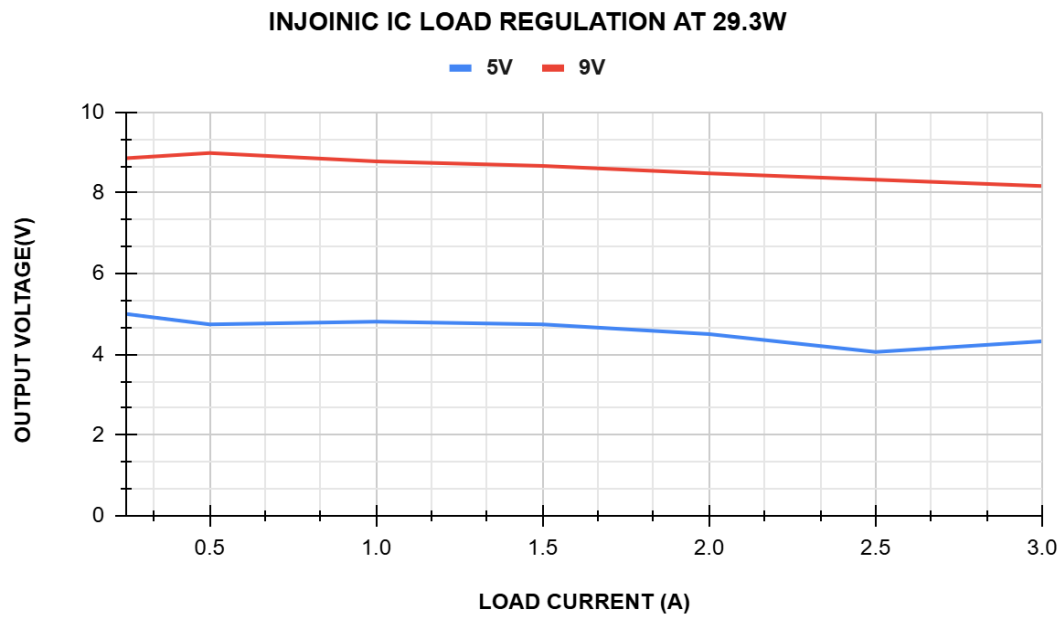

Figure 4.16: Injoinic IC Load Regulation at 29.3W

Figure 4.19 shows efficiency variation with a parallel inductor at 5V and 9V. Improved efficiency occurs at medium loads due to reduced current stress and lower conduction losses.

Further optimization used two low DCR inductors in series so that efficiency can be increased. As shown in Figure 4.20, better efficiency and load performance occurred at higher load currents due to reduced resistive losses and improved current handling.

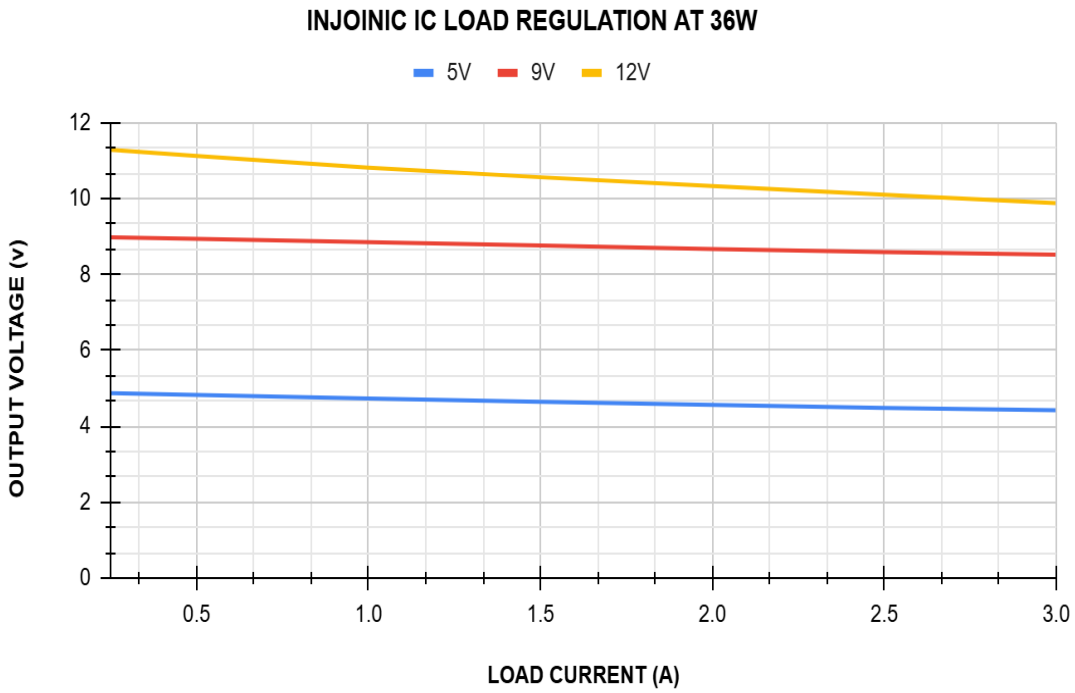

Figure 4.17: Injoinic IC Load Regulation at 36W

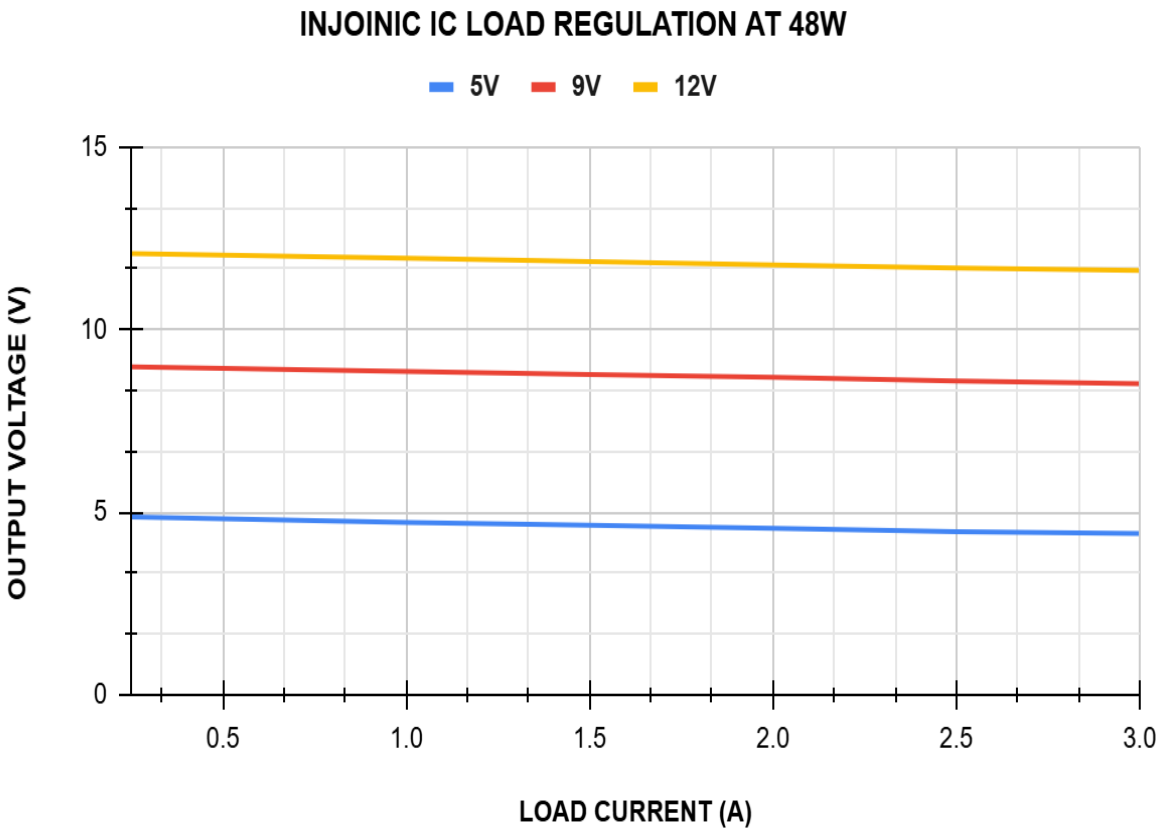

Figure 4.18: Injoinic Load Regulation at 48W

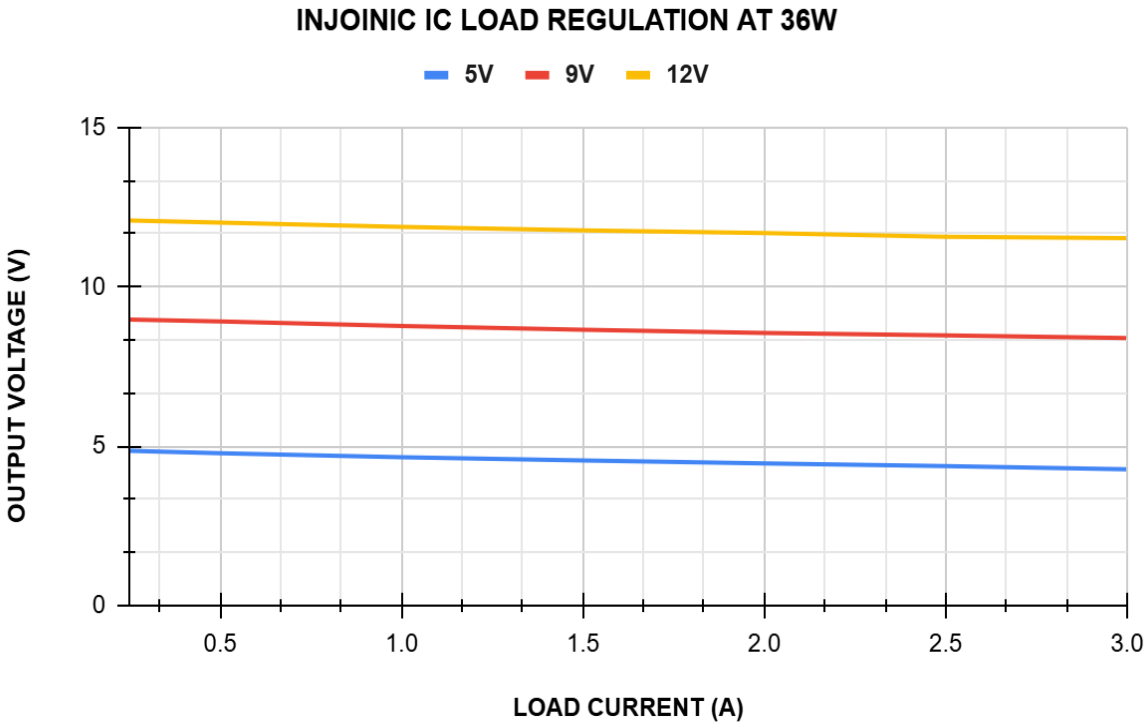

Figure 4.19: Injoinic Load Regulation at 36W (High VIN)

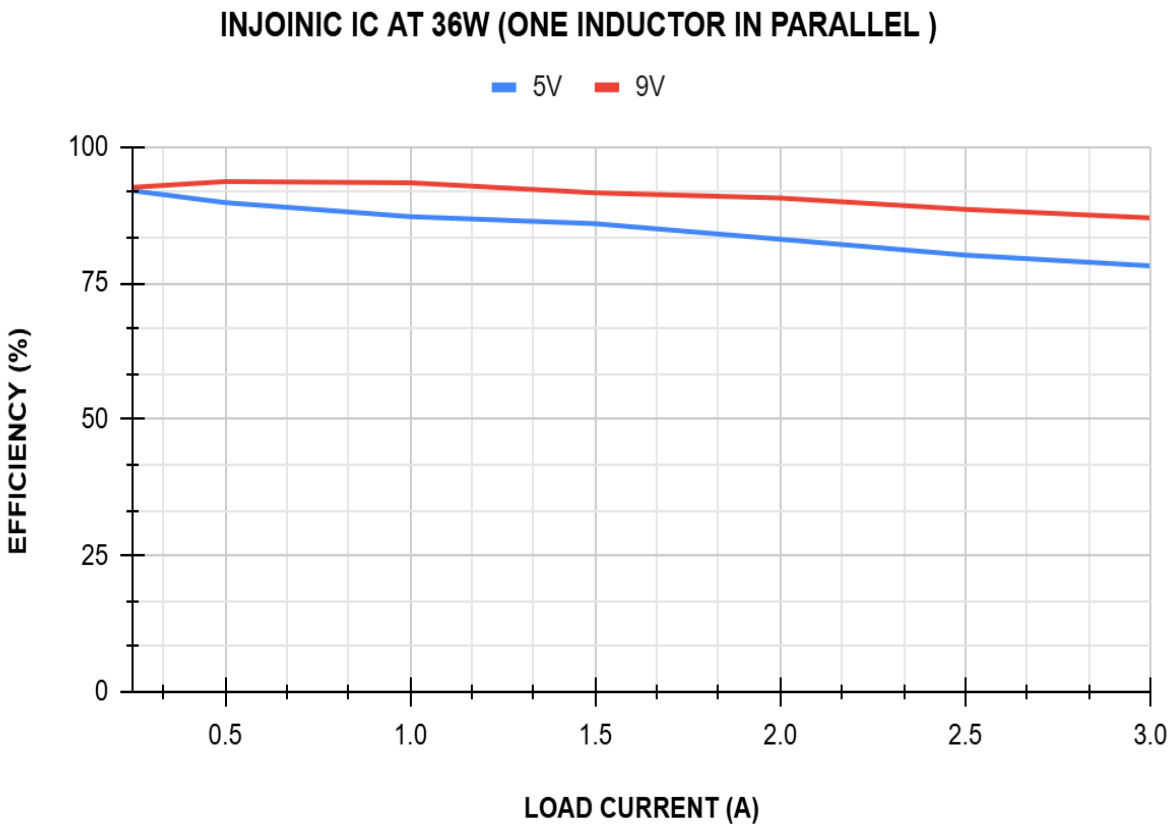

Figure 4.20: Injoinic Efficiency with Parallel Inductor Configuration

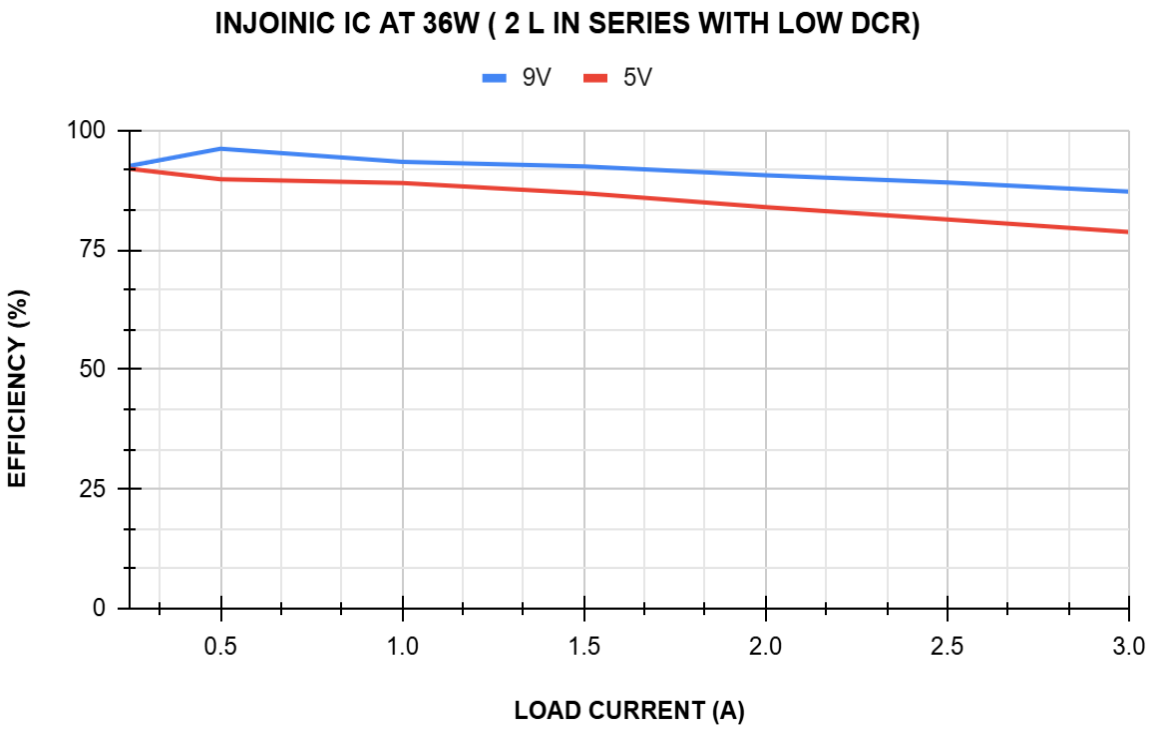

Figure 4.21: Injoinic Efficiency with Series Low DCR Inductor Configuration

4.5 Experimental Evaluation of MPS Board

Figures 5.1, 5.2, and 5.3 show the efficiency of the MPS board at 36W, 54W, and 72W. The 9V PDO profile consistently offered higher efficiency than 5V.

At 36W input (12V, 3A), the 5V profile's max efficiency was about 87.7% at 1A, while the 9V profile reached about 93.9% at 1A.

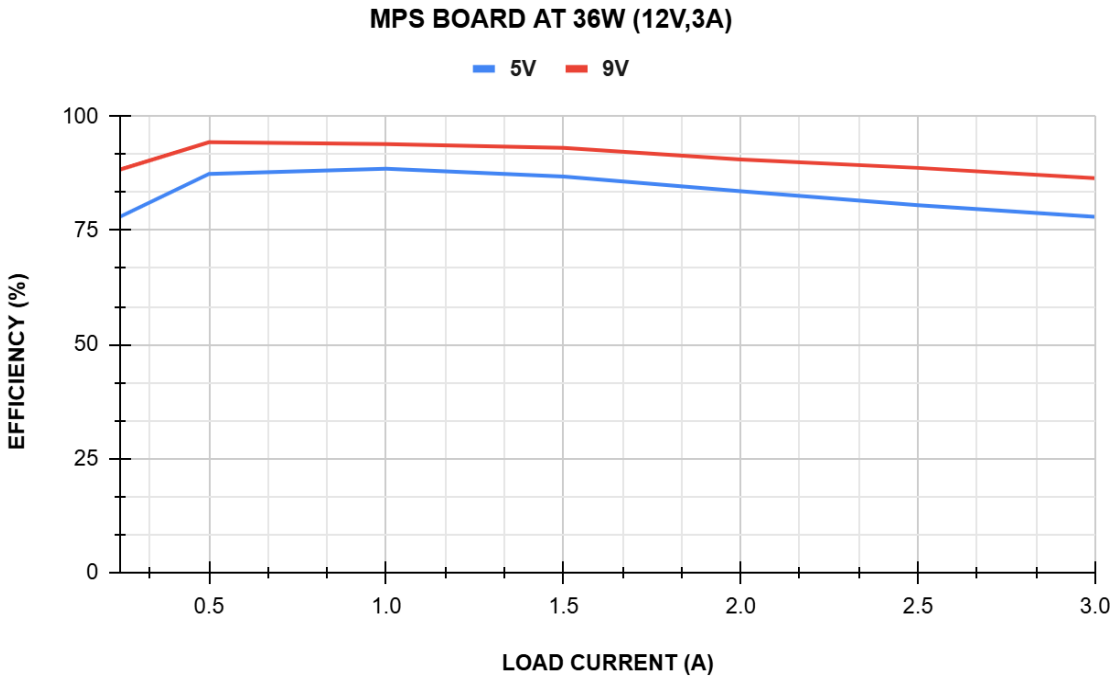

Figure 4.22: Efficiency Characteristics of MPS Board at 36W

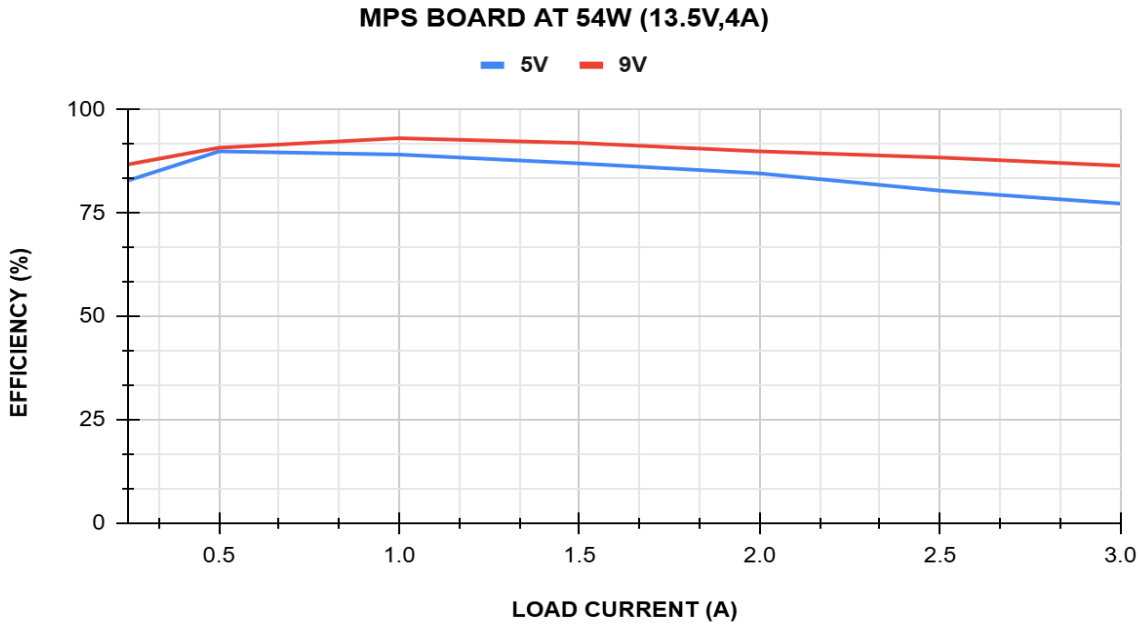

Figure 4.23: Efficiency Characteristics of MPS Board at 54W

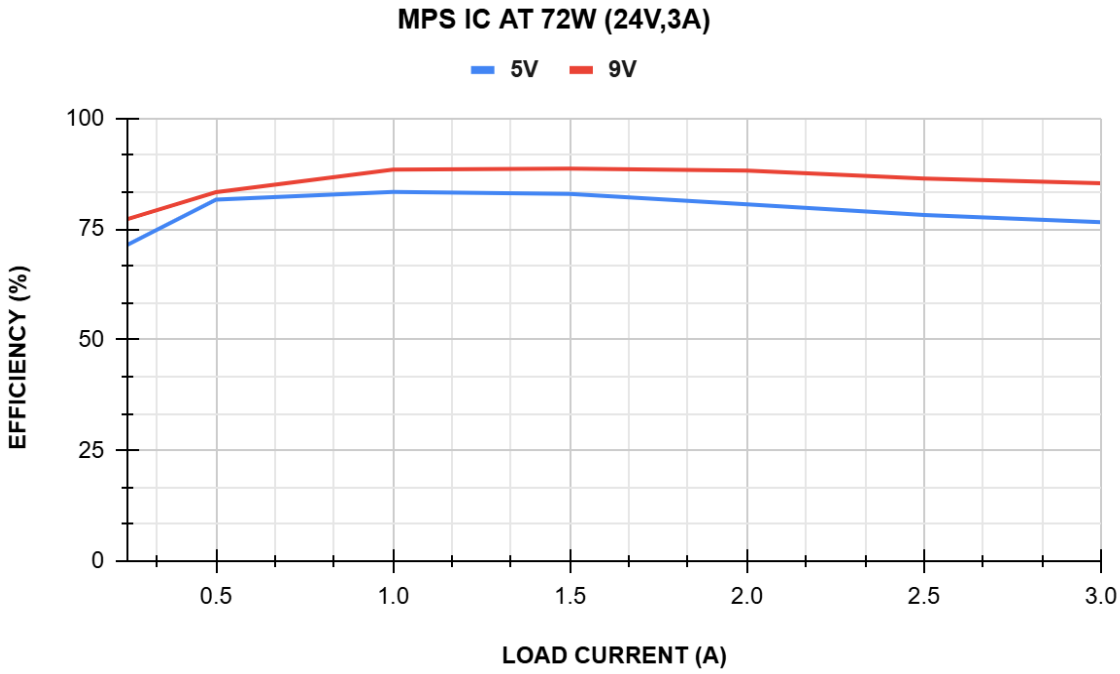

Figure 4.24: Efficiency Characteristics of MPS Board at 72W

Under an input condition of 54W (13.5V, 4A), the maximum efficiency observed for the 5V profile was approximately 87.3% at a load current of 1A, while the 9V profile achieved approximately 91.9% at the same load current.

Under 72W input (24V, 3A), the 5V profile's max efficiency drops to about 82.3% at 1A, while the 9V profile reaches about 87.6% at 1.5A.

Results show converter efficiency drops slightly at higher input voltages due to increased switching losses and efficiency rises with load current.

4.6 Load Regulation Testing for MPS Board

Figures 5.4 and 5.5 show the load regulation of the MPS board at 36W and 72W. The output voltage gradually decreases with load current for both 5V and 9V PDO profiles.

At 36W operation, the 5V output voltage decreased from approximately 4.89V to 4.05V, while the 9V output reduced from approximately 8.9V to 8.05V as the load current increased up to 3A.

During 72W operation, the 5V profile dropped from 4.89V to 4.05V, and the 9V profile from 8.9V to 8.05V under full load.

The 9V profile showed better voltage regulation due to lower current for the same power, reducing losses in MOSFETs, inductor and capacitor. Almost Stable operation occurred across all load conditions.

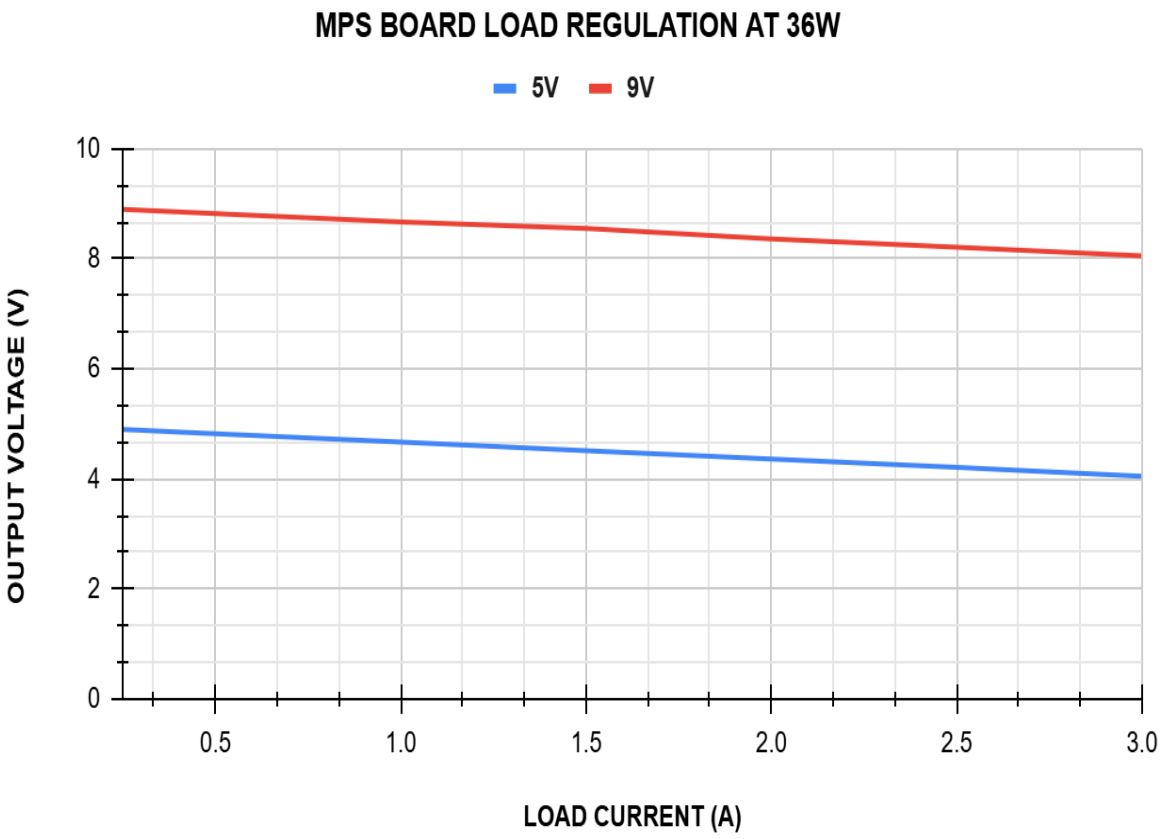

Figure 4.25: Load Regulation Characteristics of MPS Board at 36W

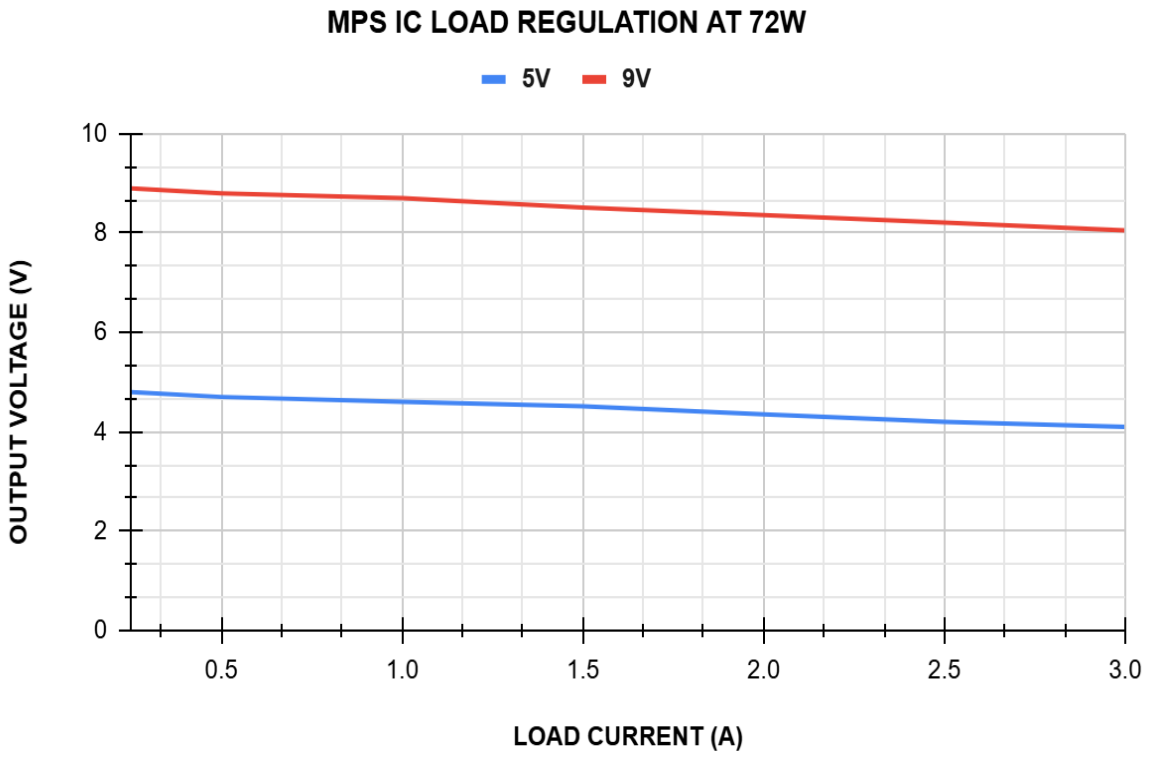

Figure 4.26: Load Regulation Characteristics of MPS Board at 72W

4.7 Experimental Evaluation of Renesas Board

Figures 4.27, 4.28, and 4.29 display the efficiency of the Renesas USB PD board at 84W, 108W, and 140W.

At 84W input (28V, 3A), the 5V profile reached about 84.5% efficiency at 1A, the 9V about 89.6%, the 15V about 91.9% at 1.5A, and the 20V the highest at 93.7% at 1A. When the system is running at 108W, which is 36V and 3A the 5V profile works best at about 82.2 % efficiency when the current is 1A.

The 9V profile does a bit better at the same current, it gets about 88.5 % efficiency. The 15V and 20V profiles do better, getting about 92.1% and 93.6% efficiency when the system is not running at full power.

When the system is running at 140W, which is 48V and 2.91A the 20V profile is the best. It gets 92.2 % efficiency when the current is 1.5A. The 15V profile gets about 90.1 %, the 9V profile gets about 85.5 percent and the 5V profile gets about 79.2 %.

The results show that the system works better when the output voltage is higher. This is because it needs current to transfer the same amount of power so there is less energy lost in the system. The 5V profile and the other profiles, like the 9V profile and the 15V profile and the 20V profile all work better when the voltage is higher.

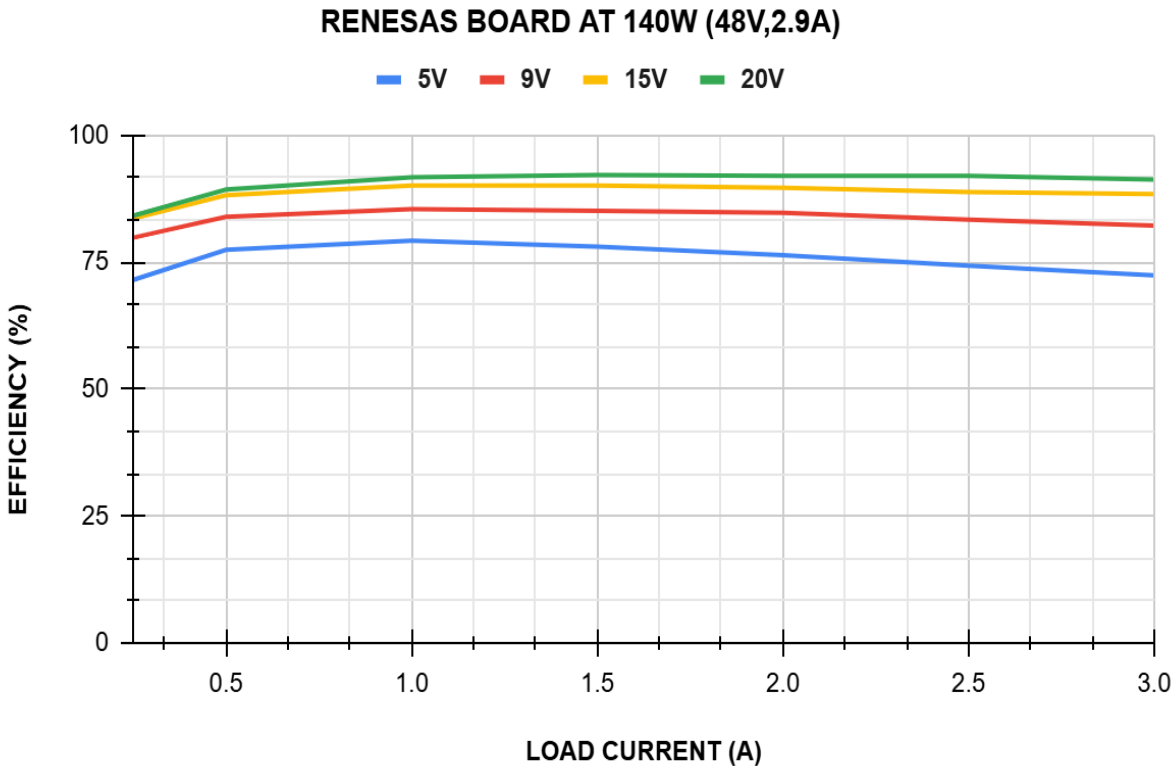

Figure 4.27: Efficiency Characteristics of Renesas Board at 84W

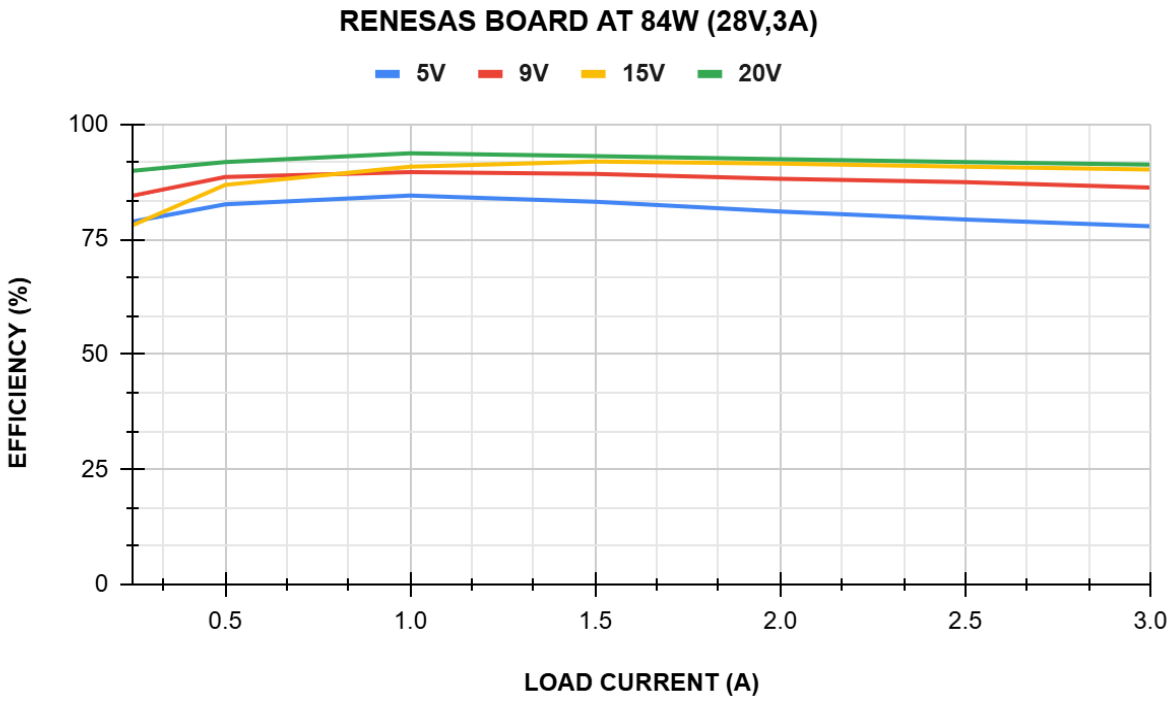

Figure 4.28: Efficiency Characteristics of Renesas Board at 108W

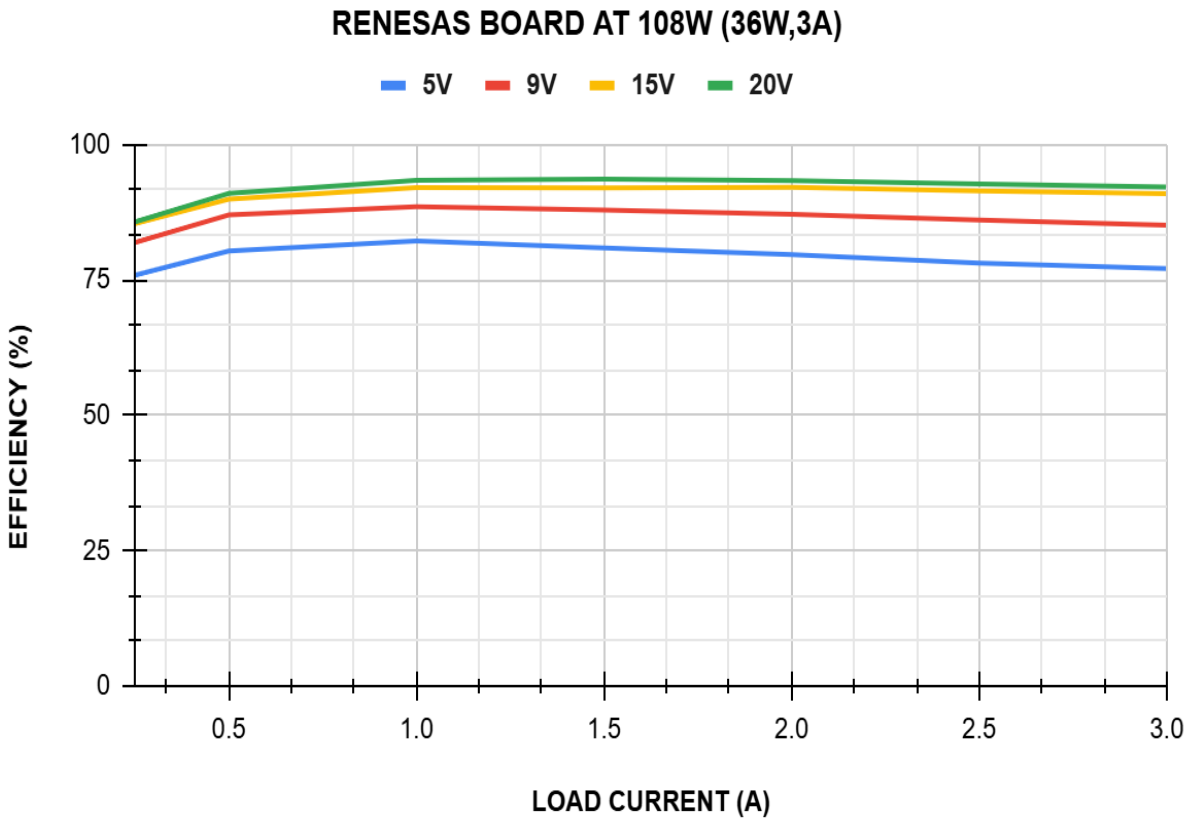

Figure 4.29: Efficiency Characteristics of Renesas Board at 140W

4.8 Load Regulation Testing for Renesas Board

Figure 4.30 and Figure 4.31 show the load regulation characteristics of the Renesas board under varying load current conditions. The output voltage gradually decreased with increasing load current for all tested PDO profiles.

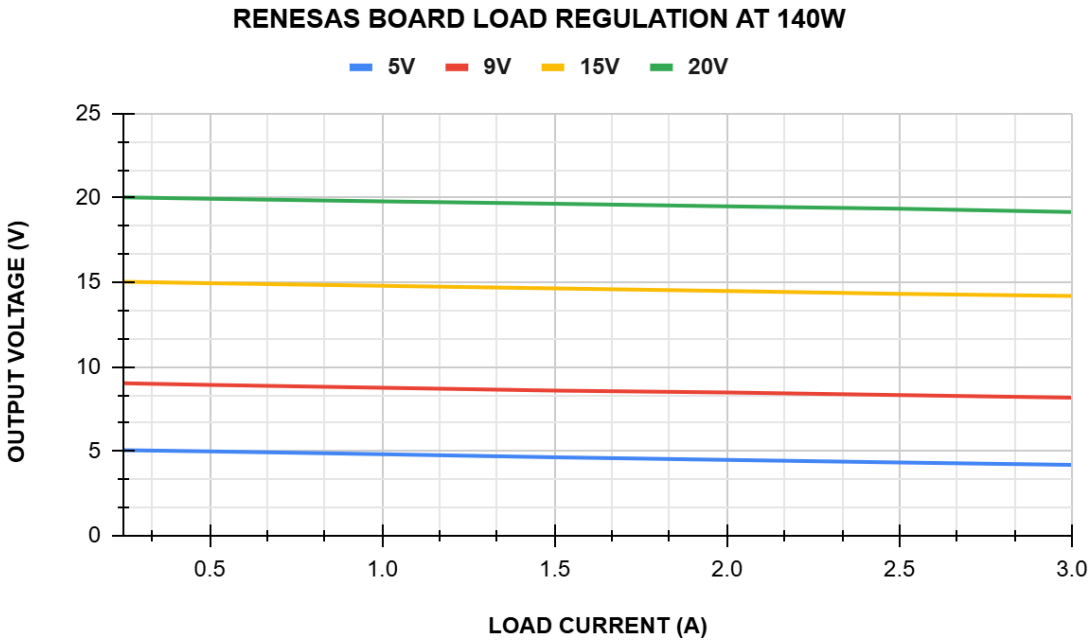

Figure 4.30: Load Regulation Characteristics of Renesas Board at 84W

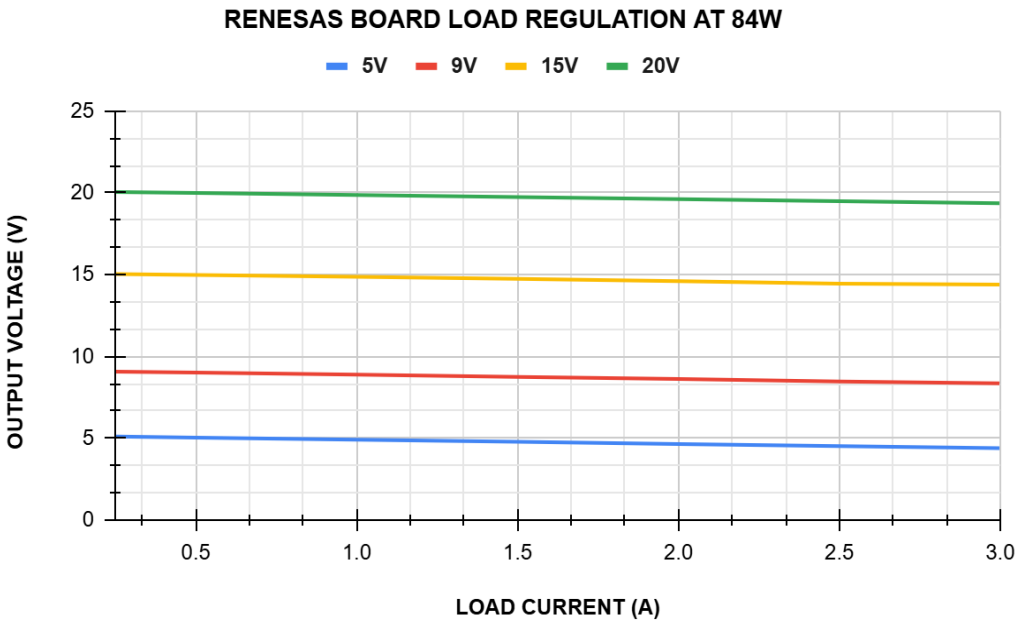

Figure 4.31: Load Regulation Characteristics of Renesas Board at 140W

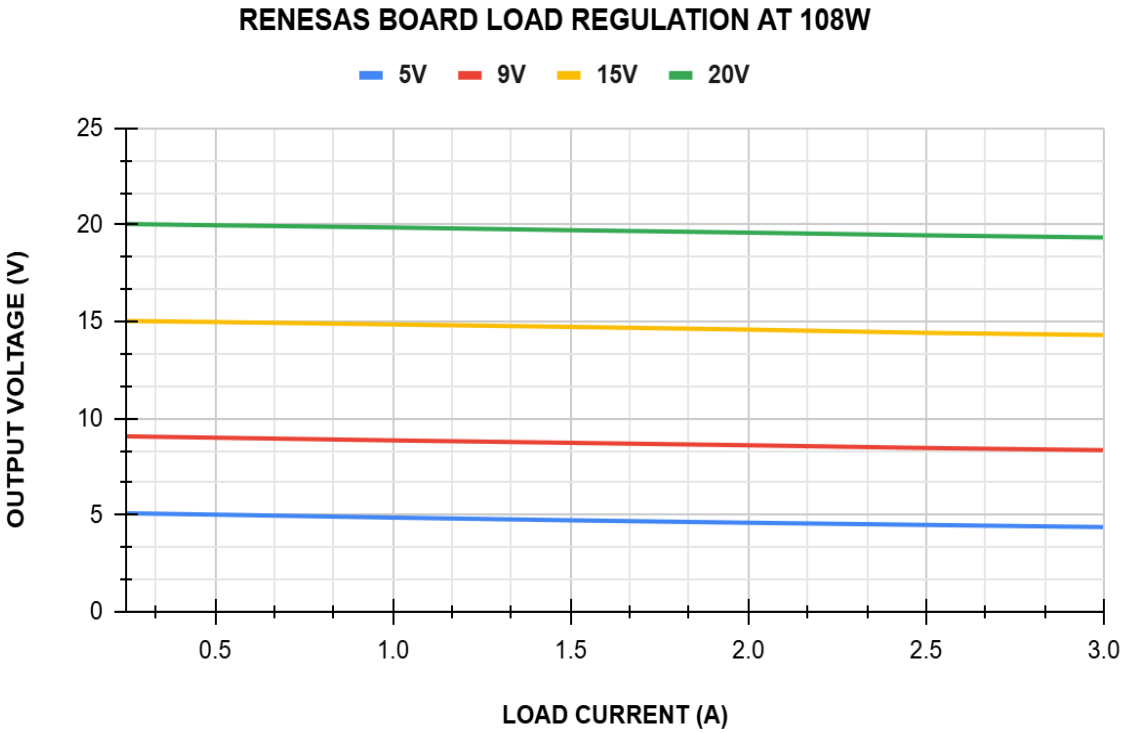

Figure 4.32: Load Regulation Characteristics of Renesas Board at 108W

During 140W operation, the 5V output voltage reduced from approximately 5.07V to 4.19V, while the 9V profile reduced from approximately 9.02V to 8.17V at full load condition. Similarly, the 15V profile decreased from approximately 15.03V to 14.2V, whereas the 20V profile reduced from approximately 20.03V to 19.17V as the load current increased up to 3A.

At 84W operation, similar load regulation behavior was observed, where higher voltage profiles showed comparatively better voltage stability than lower voltage profiles. The 20V output profile maintained the most stable regulation because lower current flow reduced conduction losses across MOSFETs, inductors.

4.9 Protection Testing

Figure 4.33 shows the Injoinic IC converter's short circuit protection. During a fault, the output voltage dropped below 4.1V, causing the IC to stop switching at the LX pin and shut down. After 2 seconds, it automatically restarted in hiccup mode.

Figure 4.33: SC Protection Response of Injoinic IC Observed on Oscilloscope

When input voltage dropped below 6.9V, the converter detected undervoltage, disabled switching at LX for 4 sec (see figure 4.34), causing output voltage zero and protection mode. Normal operation resumed once input exceeded UVP threshold.

Figure 4.34: Input UnderVoltage Protection (UVP) Response of Injoinic IC

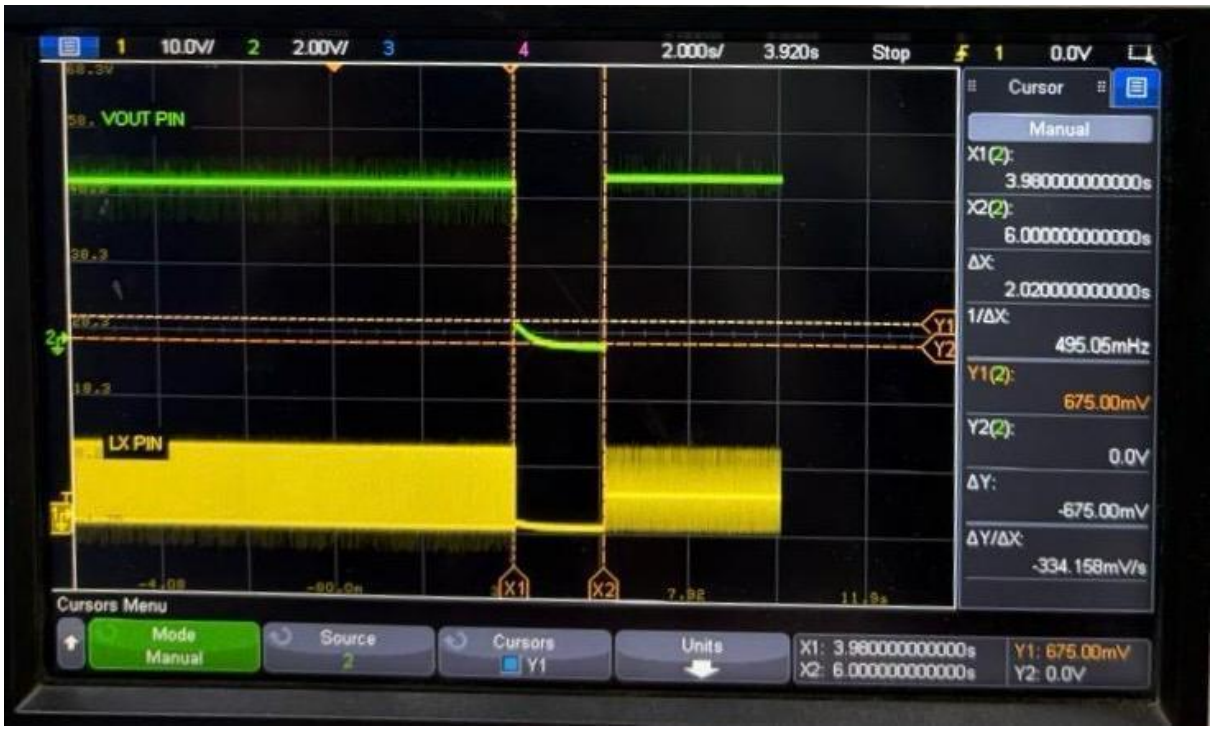

Figure 4.35: Output UVP and Hiccup Restart Response of Injoinic IC

Figure 4.35 shows that during heavy fault conditions, the output voltage fell below the 4.35 V under-voltage threshold. This caused the converter to disable the LX switching pulses for 2 sec and then restart again.

Figure 4.36: DP Pin OverVoltage Protection Response of Injoinic IC

Applying a 7.4V battery voltage to the DP pin triggered the overvoltage protection. This disturbance in the communication waveform caused the IC to go in over voltage protection of these lines. Refer to Figure 4.36.

Figure 4.37: CC Pin OverVoltage Protection Response of Injoinic IC

During CC pin protection testing, 7.4V from a battery was applied to CC1 pin. Fig 4.37 The communication waveform became unstable, and the IC stopped functioning after detecting overvoltage on the CC line.

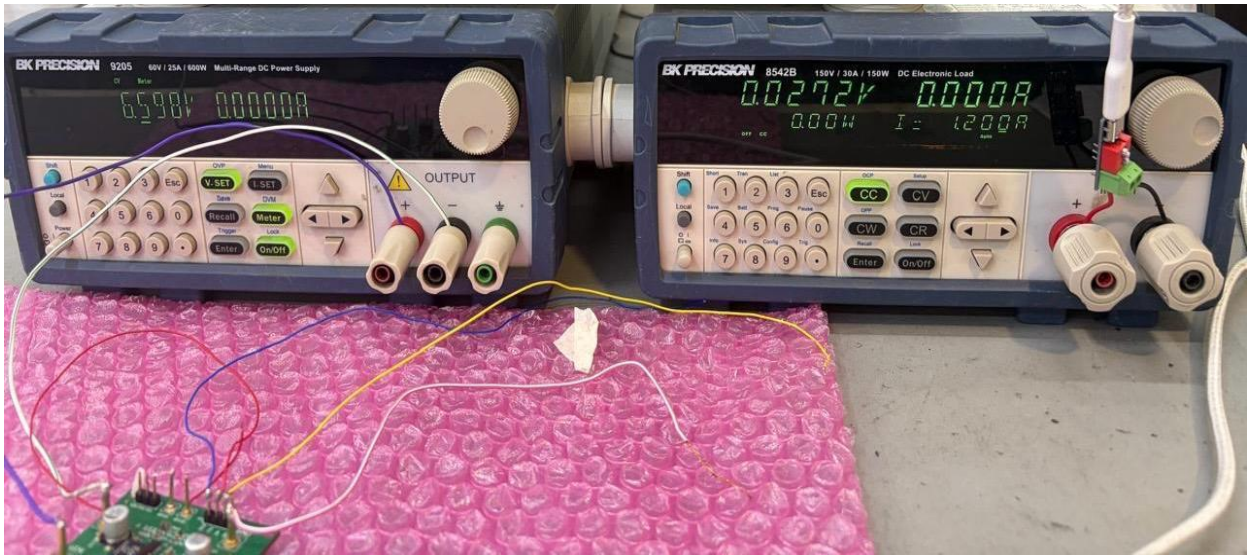

Figure 4.38: Input UnderVoltage Protection Testing of MPQ4241

During testing, the input power was lowered to 6.5V. Figure 4.38 illustrates this: at low input voltage, the converter ceased switching and disabled the output to prevent unstable operation. When the input voltage rose again, normal output function was automatically restored.

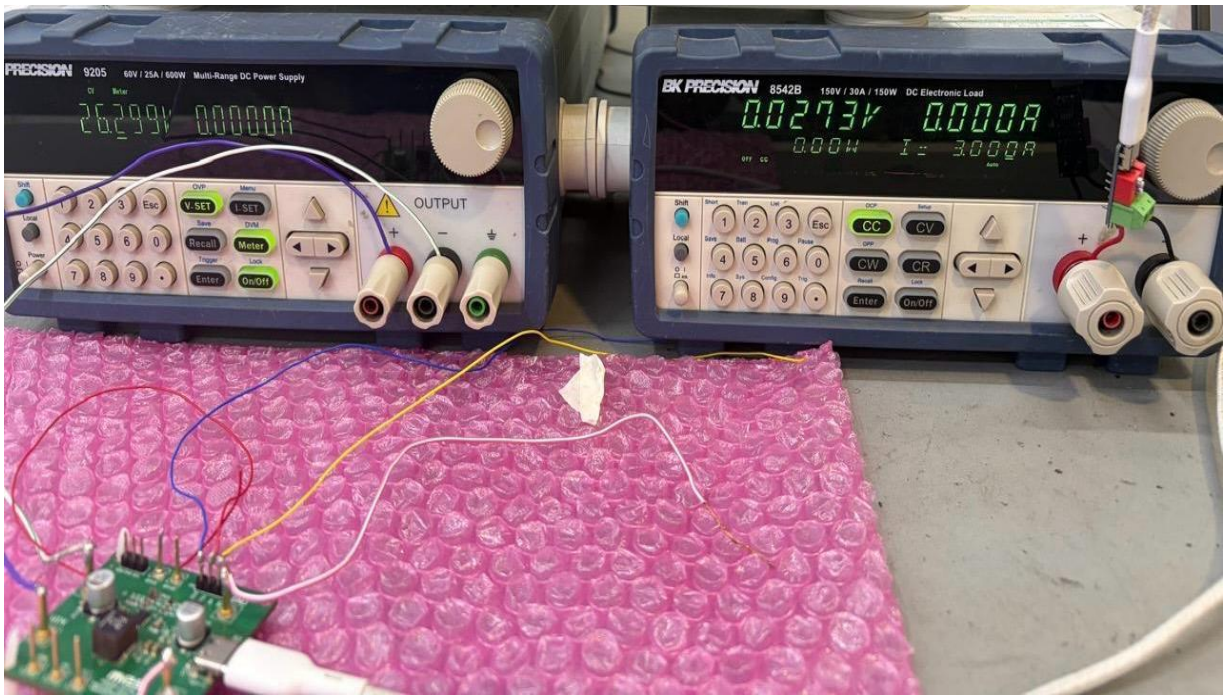

Figure 4.39: Input OverVoltage Protection Testing of MPQ4241

For OVP testing, the input voltage was raised near 27V, as shown in figure 4.39. Once it exceeded the protection limit, the IC shut down switching to protect the power stage from excessive input stress. The output automatically recovered once the input voltage was below the higher limit.

4.10 Conclusion

This chapter presented the experimental testing and performance evaluation of the selected USB PD charging s under different operating conditions.

The Injoinic demonstrated stable USB PD operation and satisfactory efficiency for compact automotive charging applications. Converter behavior was found to vary with input voltage, load condition, and passive component configuration.

The MPS demonstrated higher efficiency, better load regulation, and increased flexibility during testing. Reliable USB PD negotiation and stable PPS operation were also confirmed with the PD analyzer setup.

Initial tests on the Renesas Board showed strong high-power performance but due to hardware damage further testing was not done.

CHAPTER 5 - COMPARATIVE ANALYSIS AND CONCLUSION

5.1 Comparative Analysis of Automotive USB PD

The USB PD chargers that were tested had performance when the voltage and load were changed. The results are shown in Figures 4.1 to 4.10. Each USB PD charger had efficiency and performance when it came to heat and protection.

The Injoinic IC worked well for charging devices like scooters that do not need a lot of power. Looking at the efficiency plots the converter worked better when the voltage was higher, like 9V because it used current for the same amount of power. The Injoinic IC has everything it needs inside so it is small and easy to use in scooters.

The Figures 4.3, 4.4 and 4.5 show that the MPQ4241 board worked better when the voltage was 9V or 5V. This is because the MPQ4241 board has a special kind of converter that helps it work smoothly and reduces energy loss.

When the load was medium the output was stable and had a low ripple. When the current was high the efficiency went down a bit because of heat and energy loss.

Table 5.1: Performance Comparison of USB PD s

Parameter	**INJOINIC IC**	**MPQ4241**	**Renesas**
Power Range	36W	72W	140W
Best Efficiency Observed	89%	94%	93%
Best PDO Efficiency	9V	9V	20V
Load Regulation	Higher voltage drop at full load	Stable regulation	Better regulation at high power
Converter Topology	Integrated buck converter	Synchronous buck converter	3-level buck converter
Protection Response	Stable UVP/OVP/SCP	Programmable protections	Stable high-power protection

The load regulation is shown in Figures 4.6 and 4.7. The output voltage stayed the same when the load changed. The MPQ4241 and Renesas boards were better at keeping the voltage stable when the load was high.

This is because they have control and converter design. The Injoinic IC also worked well. The voltage dropped a bit when the load was very high.

Figures 4.8, 4.9 and 4.10 show that the converter efficiency got better when the voltage was higher, like 15V and 20V during power testing. This is because the current needed was lower for the power so the energy loss was lower. The Renesas board was very good at this because it has a 3-level converter design.

The Renesas board worked well even when the power was high up to 140W. The 3-level converter design reduced stress on the parts and improved efficiency.

The heat was also distributed well so it worked smoothly. The Renesas board is more complex than the Injoinic IC and MPQ4241 board because it needs more parts and control circuitry.

5.2 Conclusion

This work was about making and testing USB Type-C Power Delivery charger ICs that are used to charge scooter TFT displays.

We tried out chargers with different voltages and loads to see how they worked, what protocols they supported, how efficient they were and how well they were protected.

When we were testing, we were able to get the USB PD communication working with the help of some tools. We checked out voltage options like 5V, 9V, 15V and 20V to see how they did with real loads.

What we found out was that how well the converter worked depended on things like the switching setup, how hot it got, the parts used and the voltage.

The Injoinic IC was a choice for charging TFT displays because it was small and easy to use, and it had good protection. The MPQ4241 board was flexible because you could change the USB PD settings, and it supported PPS.

The Renesas board was good at handling power because it had a special 3-level converter that reduced losses when it was working hard.What we learned from all this was that using voltages made the chargers work better by reducing stress and losses.

We also saw that it is really important to test the hardware in life because it can work differently than what the specs say. USB Type-C Power Delivery charger ICs, like these, are used for scooter TFT display charging applications. We need to make sure they work well.

5.3 Future Scope

We can work on looking at how the scooter's electronics affect each other and how they work when they get hot. We should test the scooter's parts when it is being used for a while to see if they still work well.

We can also see how the scooter's parts work when they are being shaken around, charged for a time and used in different environments. This will help us make sure the scooter works well in life.

In the future we might try to make the scooters charging system work with better technology like USB PD 3.1 Extended Power Range. This would let us charge the scooter's battery faster and more safely.

REFERENCE

[1] USB Implementers Forum, “USB Power Delivery Specification Revision 3.1,” USB-IF Standard, Jan. 2021.

[2] USB Implementers Forum, “Universal Serial Bus Type-C Cable and Connector Specification Revision 2.1,” USB-IF Standard, May 2021.

[3] S. Dusmez and A. Khaligh, “A Compact and Integrated Multifunctional Power Electronic Interface for Plug-In Electric Vehicles,” IEEE Transactions on Power Electronics, vol. 28, no. 12, pp. 5690–5701, Dec. 2013.

[4] K. Yao, Y. Ren, and F. C. Lee, “Critical Conduction Mode Buck Converter With Lossless Current Sensing for USB Power Delivery Applications,” IEEE Transactions on Power Electronics, vol. 34, no. 10, pp. 9913–9924, Oct. 2019.

[5] B. Bryant and M. K. Kazimierczuk, “Voltage Loop Power-Stage Transfer Functions With MOSFET Delay for Buck PWM Converter Operating in CCM,” IEEE Transactions on Industrial Electronics, vol. 54, no. 1, pp. 347–353, Feb. 2007.

[6] Y. Liu, X. Zhang, and H. Wang, “Research and Design of Fast Charge Controller Based on USB-PD Protocol of FPGA,” Journal of Physics: Conference Series, vol. 1639, no. 1, 2020, doi: 10.1088/1742-6596/1639/1/012005.

[7] Siamak Delshadpour, Abhijeet Kulkarni, and Xu Zhang, “A BMC Analog and Digital PHY for USB Type-C Power Delivery,” Canadian Journal of Electrical and Computer Engineering, vol. 43, no. 3, pp. 195–202, Summer 2020, doi: 10.1109/CJECE.2020.3007200.

[8] Satyaki Mukherjee, Ashish Kumar, and Dragan Maksimovic, “Efficiency-Optimized Current-Source Resonant Converter for USB-C Power Delivery,” in Proc. IEEE Applied Power Electronics Conference and Exposition (APEC), 2021, pp. 1548–1555.

[9] Thanh Nhat Trung Tran, Jian-Min Wang, Ching-Chun Chuang, and Sen-Tung Wu, “Design of Battery Charger With USB Type-C Power Delivery Interface,” in Proc. IEEE 11th International Conference on Power Electronics and ECCE Asia (ICPE 2023-ECCE Asia), Jeju, Korea, 2023, pp. 221–226.

[10] Hong Cai and Yong Liu, “Adaptive USB Fast Charger Design Based on Quick Charge 2.0 Protocol,” Advanced Materials Research, vol. 852, pp. 357–360, 2014, doi: 10.4028/www.scientific.net/AMR.852.357.

[11] Injoinic Technology Co., Ltd., “IP6520/INJOINIC IC USB Type-C and PD Fast Charging SOC Datasheet,” Injoinic Technology, 2024.

[12] Monolithic Power Systems, “MPQ4241-AEC1: 65W Fully Integrated USB Type-C Power Delivery Solution Datasheet,” Monolithic Power Systems Inc., 2025.

[13] Renesas Electronics Corporation, “RAA489300 3-Level Buck Controller with Passthrough Mode Datasheet,” Renesas Electronics, 2025.

[14] Renesas Electronics Corporation, “RAA489400 USB Type-C Port Controller Datasheet,” Renesas Electronics, 2025.

[15] Tianshi Xie and Hanh-Phuc Le, “A Zero-Voltage-Switching 3-Level Buck Converter Achieving 30% Loss Reduction at Light Load for USB-C Charger Applications,” in Proc. IEEE Applied Power Electronics Conference and Exposition (APEC), 2023, pp. 932–936, doi: 10.1109/APEC43580.2023.10131344.

[16] Przemysław Ptak, Tadeusz Lorkowski, and Krzysztof Górecki, “Influence of the Type of Load on Characteristics of a Dedicated USB PD Charging System—A Case Study,” Applied Sciences, vol. 15, no. 10, p. 5254, 2025, doi: 10.3390/app15105254.

[17] S. Choi, T. Kim, and J. Yang, “Thermal Analysis of High-Power USB Fast Charging Systems,” IEEE Access, vol. 8, pp. 178321–178330, 2020.

[18] H. Matsuda and K. Ito, “Analysis of Conducted EMI Noise in High-Frequency DC–DC Buck Converters,” in Proc. IEEE International Symposium on Electromagnetic Compatibility, 2018, pp. 412–417.

[19] Tianyu Zhao, Rolando Burgos, Bo Wen, Andrew McLean, and Rodrigo Fernandez Mattos, “Hardware Design Considerations for a 100 W USB Type-C Power Delivery in Aircraft Application,” in Proc. IEEE Energy Conversion Congress and Exposition (ECCE), 2023, pp. 1–5, doi: 10.1109/ECCE59906.2023.10345783.

[20] Yinglyu Xiong, Yong Zhou, Ruichen Wang, Zehao Tao, Xun Liu, and Ka Leung, “A Multi-Mode Step-Up/Down Hybrid Converter With Always Reduced Inductor Current for USB PD 3.1 Standard in EV Applications,” IEEE Journal of Emerging and Selected Topics in Power Electronics, Early Access, 2025, doi: 10.1109/JESTPE.2025.3640286.

[21] Simon Kim, Lucas Park, Ryan Lee, Kevin Kim, and Peter Han, “Design Proposal Using USB PD Controller for Power Extension and Circuit Compactness in USB Type-C Power Delivery Applications,” in Proc. International Conference on Electrical Machines and Systems (ICEMS), 2025, pp. 1302–1305, doi: 10.23919/ICEMS66262.2025.11317651.

[22] Monolithic Power Systems, “EVQ4241-LE-00A Evaluation Board User Guide for MPQ4241 USB PD Solution,” Monolithic Power Systems Inc., Nov. 2023.

[23] Injoinic Technology Co., Ltd., “IP6520U USB Type-C PD3.1/PPS Fast Charging Solution Datasheet and Application Information,” Injoinic Technology, 2025.

[24] Renesas Electronics Corporation, “RAA489300 High-Performance Three-Level Buck Controller for USB-C Power Systems,” Renesas Electronics Datasheet, Oct. 2025.

[25] Renesas Electronics Corporation, “RAA489400 USB Type-C Port Controller Supporting USB PD 3.1 and EPR Operation,” Renesas Electronics, 2025.

[26] R. W. Erickson and D. Maksimovic, Fundamentals of Power Electronics, 2nd ed. New York, NY, USA: Springer, 2001.

[27] H. Wang and F. Blaabjerg, “Reliability of Power Electronic Converters in Renewable Energy Systems,” IEEE Transactions on Power Electronics, vol. 28, no. 6, pp. 2967–2978, Jun. 2013.

[28] R. W. Erickson and D. Maksimovic, Fundamentals of Power Electronics, 2nd ed. New York, NY, USA: Springer, 2001.

[29] H. Wang and F. Blaabjerg, “Reliability of Power Electronic Converters in Renewable Energy Systems,” IEEE Transactions on Power Electronics, vol. 28, no. 6, pp. 2967–2978, Jun. 2013.

Chitresh Shahi

24ci22Dhratika singh-1

Document Details

Submission ID
trn:oid:::27535:142464384

Submission Date
Jun 10, 2026, 1:54 PM GMT+0

Download Date
Jun 16, 2026, 11:01 AM GMT+0

File Name
24ci22Dhratika singh-1.pdf

File Size
4.2 MB

59 Pages

11,062 Words

62,672 Characters

0% Overall Similarity

The combined total of all matches, including overlapping sources, for each database.

Filtered from the Report

- Small Matches (less than 14 words)

Exclusions

- 10 Excluded Matches

Match Groups

1 Not Cited or Quoted 0%
Matches with neither in-text citation nor quotation marks

0 Missing Quotations 0%
Matches that are still very similar to source material

0 Missing Citation 0%
Matches that have quotation marks, but no in-text citation

0 Cited and Quoted 0%
Matches with in-text citation present, but no quotation marks

Top Sources

0% Internet sources
0% Publications
0% Submitted works (Student Papers)

Integrity Flags

0 Integrity Flags for Review

Our system's algorithms look deeply at a document for any inconsistencies that would set it apart from a normal submission. If we notice something strange, we flag it for you to review.

A Flag is not necessarily an indicator of a problem. However, we'd recommend you focus your attention there for further review.